CHAPTER

# 3 The Characteristic-Based Split (CBS) Algorithm: A General Procedure for Compressible and Incompressible Flow

## 3.1 Introduction

In the first chapter we have written the fluid dynamics equations in a very general format applicable to both incompressible and compressible flows. The equations included that of energy which for compressible situations are fully coupled with equations for conservation of mass and momentum. However, of course, the equations, with small modifications, are applicable for specialized treatment in scenarios from incompressible flow where the energy coupling disappears, to the problems of shallow-water equations where the variables describe a somewhat different flow regime. Chapters 4–6 and 10 deal with such specialized forms.

The equations have been written in Chapter 1 in fully conservative, standard form [Eqs. (1.25) and (1.26a)–(1.26d)] but all the essential features can be captured by writing the three sets of equations as below.

*Mass conservation*

$$\frac{\partial \rho}{\partial t} = -\frac{\partial U_i}{\partial x_i} \tag{3.1}$$

For flows with small compressibility (see Eq. 1.44c)

$$\frac{\partial \rho}{\partial t} = \frac{1}{c^2}\frac{\partial p}{\partial t} = -\frac{\partial U_i}{\partial x_i} \tag{3.2}$$

where $c$ is the speed of sound and depends on $E$, $p$, and $\rho$ and, assuming constant entropy,

$$c^2 = \frac{\partial p}{\partial \rho} = \frac{\gamma p}{\rho} \tag{3.3}$$

where $\gamma$ is the ratio of specific heats equal to $c_p/c_v$, where $c_p$ is the specific heat at constant pressure and $c_v$ is the specific heat at constant volume, and we define the mass flow flux as

$$U_i = \rho u_i \tag{3.4}$$

**Finite Element Meth Fluid Dynam 7E, Volume 3.** http://dx.doi.org/10.1016/B978-1-85617-635-4.00003-0

For a fluid with a small compressibility, the speed of sound may be written as

$$c^2 = \frac{K}{\rho} \tag{3.5}$$

in which $K$ is the elastic bulk modulus. Depending on the application we use an appropriate relation for $c^2$.

*Momentum conservation*

$$\frac{\partial U_i}{\partial t} = -\frac{\partial}{\partial x_j}(u_j U_i) + \frac{\partial \tau_{ij}}{\partial x_j} - \frac{\partial p}{\partial x_i} + \rho g_i \tag{3.6}$$

*Energy conservation*

$$\frac{\partial(\rho E)}{\partial t} = -\frac{\partial}{\partial x_i}(u_i \rho E) + \frac{\partial}{\partial x_i}\left(k\frac{\partial T}{\partial x_i}\right) - \frac{\partial}{\partial x_i}(u_i p) + \frac{\partial}{\partial x_i}(\tau_{ij} u_j) + \rho g_i u_i \tag{3.7}$$

In all of the above $u_i$ are the velocity components, $\rho$ is the density, $E$ is the specific energy, $p$ is the pressure, $T$ is the absolute temperature, $\rho g_i$ represents body forces and other source terms, $k$ is the thermal conductivity, and $\tau_{ij}$ are the deviatoric stress components given by (Eq. 1.11b)

$$\tau_{ij} = \mu\left(\frac{\partial u_i}{\partial x_j} + \frac{\partial u_j}{\partial x_i} - \tfrac{2}{3}\delta_{ij}\frac{\partial u_k}{\partial x_k}\right) \tag{3.8}$$

where $\delta_{ij}$ is the Kronecker delta and equals 1 if $i = j$ and 0 if $i \neq j$. In general, $\mu$, the dynamic viscosity, in the above equation is a function of temperature, $\mu(T)$, and appropriate relations will be used if necessary. The equations are completed by a relationship that relates the pressure and density. One of the popular choices of this relation is the universal gas law when the flow is coupled and compressible, i.e.,

$$p = \rho R T \tag{3.9}$$

where $R$ is the universal gas constant.

The reader will observe that the major difference in the momentum-conservation equation (3.6) and the corresponding ones describing the behavior of solids (see Ref. [1]) is the presence of a convective acceleration term.

This does not lend itself to the optimal Galerkin approximation as the equations are now non-self-adjoint in nature (see Appendix A). However, it will be observed that if a certain split is made, the characteristic-Galerkin procedure can be applied to the part of the system which is not self-adjoint but has an identical form to the convection-diffusion equation. We have shown in the previous chapter that the characteristic-Galerkin procedure is excellent for dealing with such equations. However, we have also shown that many alternatives will lead to precisely the same convection stabilizing terms. The choice of the name CBS is thus somewhat subjective indicating simply that the characteristic process is, for us, the most basic justification.

It is important to state again here that the equations given above are of the conservation forms. As it is possible for nonconservative equations (Appendix B) to yield multiple and/or inaccurate solutions, this fact is very important.

*We believe that the algorithm introduced in this chapter is currently the most general one available for fluids, as it can be directly applied to almost all physical situations*. We shall show such applications ranging from low Mach number viscous or indeed inviscid flow to the solution of hypersonic flows. In all applications the algorithm proves to be at least as good as other procedures developed. Further, in problems of very slow viscous flow we find that the treatment can be almost identical to that of incompressible elastic solids and here we shall often find it expedient to use higher-order approximations satisfying the incompressibility conditions (the so-called Babuška-Brezzi restriction) [2,3]. Indeed on certain occasions the direct use of incompressibility stabilizing processes is as described in Chapter 10 of Ref. [1].

## 3.2 Nondimensional form of the governing equations

The governing equations described above, Eqs. (3.1)–(3.9), are often written in nondimensional form. The scales used to nondimensionalize these equations vary depending on the nature of the flow. We describe below the scales frequently used in flow computations, though of course many alternatives are possible:

$$\begin{aligned} \bar{t} &= \frac{t u_\infty}{L}, \quad \bar{x}_i = \frac{x_i}{L}, \quad \bar{\rho} = \frac{\rho}{\rho_\infty}, \quad \bar{p} = \frac{p}{\rho_\infty u_\infty^2} \\ \bar{u}_i &= \frac{u_i}{u_\infty}, \quad \bar{E} = \frac{E}{u_\infty^2}, \quad \bar{T} = \frac{T c_p}{u_\infty^2}, \quad \bar{c}^2 = \frac{c^2}{u_\infty^2} \end{aligned} \tag{3.10}$$

where an overbar indicates a nondimensional quantity, subscript $\infty$ represents a free stream quantity, and $L$ is a reference length. Applying the above scales to the governing equations and rearranging we have the following form:

*Conservation of mass*

$$\frac{\partial \bar{\rho}}{\partial \bar{t}} = -\frac{\partial \bar{U}_i}{\partial \bar{x}_i} \tag{3.11}$$

*Conservation of momentum*

$$\frac{\partial \bar{U}_i}{\partial \bar{t}} = -\frac{\partial}{\partial \bar{x}_j}(\bar{u}_j \bar{U}_i) + \frac{1}{Re}\frac{\partial (\bar{\nu}\bar{\tau}_{ij})}{\partial \bar{x}_j} - \frac{\partial \bar{p}}{\partial \bar{x}_i} + \bar{\rho}\,\bar{g}_i \tag{3.12}$$

where

$$Re = \frac{u_\infty L}{\nu_\infty}, \qquad \bar{g}_i = \frac{g_i L}{u_\infty^2}, \qquad \bar{\nu} = \frac{\nu}{\nu_\infty} \tag{3.13}$$

are the Reynolds number, nondimensional body forces, and viscosity ratio, respectively. In the above equation $\nu$ is the kinematic viscosity equal to $\mu/\rho$ with $\mu$ being the dynamic viscosity.

*Conservation of energy*

$$\frac{\partial(\bar{\rho}\bar{E})}{\partial\bar{t}} = -\frac{\partial}{\partial\bar{x}_i}(\bar{u}_i\bar{\rho}\bar{E}) + \frac{1}{RePr}\frac{\partial}{\partial\bar{x}_i}\left(k^\star\frac{\partial\bar{T}}{\partial\bar{x}_i}\right) - \frac{\partial}{\partial\bar{x}_i}(\bar{u}_j\bar{p}) + \frac{1}{Re}\frac{\partial}{\partial\bar{x}_i}(\bar{\nu}\bar{\tau}_{ij}\bar{u}_j) \tag{3.14}$$

where $Pr$ is the Prandtl number and $k^\star$ is the conductivity ratio given by the relations

$$Pr = \frac{\mu_\infty c_p}{k_\infty}, \qquad k^\star = \frac{k}{k_\infty} \tag{3.15}$$

where $k_\infty$ is a reference thermal conductivity.

*Equation of state*

$$\bar{p} = \frac{\bar{\rho}R\bar{T}}{c_p} = \bar{\rho}\bar{R}\bar{T} = \bar{\rho}\frac{(\gamma-1)}{\gamma}\bar{T} \tag{3.16}$$

In the above equation $R = c_p - c_v$ and $\bar{R} = (c_p - c_v)/c_p$ are used. The following forms of nondimensional equations are useful to relate the speed of sound, temperature, pressure, energy, etc.

$$\begin{aligned}
\bar{E} &= \frac{\bar{T}}{\gamma} + \tfrac{1}{2}\bar{u}_i\bar{u}_i \\
\bar{c}^2 &= (\gamma-1)\bar{T} \\
\bar{p} &= (\gamma-1)\left(\bar{\rho}\bar{E} - \tfrac{1}{2}\frac{\bar{U}_i\bar{U}_i}{\bar{\rho}}\right)
\end{aligned} \tag{3.17}$$

The above nondimensional equations are convenient when coding the CBS algorithm. However, the dimensional form will be retained in this and other chapters for clarity.

## 3.3 Characteristic-based split (CBS) algorithm

### 3.3.1 The split: General remarks

The split follows the process initially introduced by Chorin [4,5] for incompressible flow problems in a finite difference context. A similar extension of the split to a finite element formulation for different applications of incompressible flows has been carried out by many authors [6–34]. However, in this chapter we extend the split to solve the fluid dynamics equations of both compressible and incompressible forms using the characteristic-Galerkin procedure [35–87]. The algorithm in its full form was first introduced in 1995 by Zienkiewicz and Codina [35,36] and followed several years of preliminary research [88–92].

Although the original Chorin split [4,5] could never be used in a fully explicit algorithm, the new form is applicable for fully compressible flows in both explicit and semi-implicit forms. The split provides a fully explicit algorithm even in the

incompressible case for steady-state problems now using an "artificial" compressibility which does not affect the steady-state solution; unsteady state can be recovered through so-called dual time stepping [57]. When real compressibility exists, such as in gas flows, the computational advantages of the explicit form compare well with those of other currently used schemes and the additional cost due to splitting is insignificant. Generally for an identical cost, results are considerably improved throughout a large range of aerodynamic problems. However, a further advantage is that both subsonic and supersonic problems can be solved by the same algorithm.

### 3.3.2 The split: Temporal discretization

At this stage we will only consider the solution of (3.1) and (3.6) with variables $u_i$ and $p$. The extension to include energy and any other variables will be treated after these are available. We can discretize Eq. (3.6) in time using the characteristic-Galerkin process. Except for the pressure term this equation is similar to the convection-diffusion equation (2.11). This term can however be treated as a known (source type) quantity provided we have an independent way of evaluating the pressure. Before proceeding with the algorithm, we repeat Eq. (3.6) below for use with the characteristic-Galerkin method:

$$\frac{\partial U_i}{\partial t} = -\frac{\partial}{\partial x_j}(u_j U_i) + \frac{\partial \tau_{ij}}{\partial x_j} - \frac{\partial p}{\partial x_i} + \rho g_i \tag{3.18}$$

At this stage we have to introduce the "split" in which we substitute a suitable approximation. In all procedures the values of the solution $(U_i^{n+1}, p^{n+1})$ at time $t^{n+1}$ must be determined from the known values $(U_i^n, p^n)$ at time $t^n$. Two alternative approximations are useful and we shall describe these as *Split A* and *Split B*, respectively. In each we assume during the time increment $\Delta t = t^{n+1} - t^n$

$$U_i^{n+1} = U_i^n + \Delta U_i^\star + \Delta U_i^{\star\star} \tag{3.19}$$

We also discretize in time using the approximation for the time interval $t^n \le t \le t^{n+1}$

$$\frac{\partial U_i}{\partial t} = \frac{U_i^{n+1} - U_i^n}{\Delta t} = \frac{\Delta U_i^\star}{\Delta t} + \frac{\Delta U_i^{\star\star}}{\Delta t} \tag{3.20}$$

Using Eq. (2.105) from the previous chapter and replacing $\phi$ by $U_i$, we can write

$$\begin{aligned} U_i^{n+1} - U_i^n = \Delta t\left[ -\frac{\partial}{\partial x_j}(u_j U_i)^n + \frac{\partial \tau_{ij}^n}{\partial x_j} + (\rho g_i)^n \right] - \Delta t \frac{\partial p^{n+\theta_2}}{\partial x_i} \\ + \frac{\Delta t^2}{2} u_k \frac{\partial}{\partial x_k}\left[ \frac{\partial}{\partial x_j}(u_j U_i) - \frac{\partial \tau_{ij}^n}{\partial x_j} - \rho g_i \right]^n \\ + \frac{\Delta t^2}{2} u_k \frac{\partial}{\partial x_k}\left( \frac{\partial p^{n+\theta_2}}{\partial x_i} \right) \end{aligned} \tag{3.21}$$

In the above equation

$$\frac{\partial p^{n+\theta_2}}{\partial x_i} = (1-\theta_2)\frac{\partial p^n}{\partial x_i} + \theta_2 \frac{\partial p^{n+1}}{\partial x_i} \tag{3.22}$$

or

$$\frac{\partial p^{n+\theta_2}}{\partial x_i} = \frac{\partial p^n}{\partial x_i} + \theta_2 \frac{\partial \Delta p}{\partial x_i} \tag{3.23}$$

where

$$\Delta p = p^{n+1} - p^n \tag{3.24}$$

The reader should note that the velocity and deviatoric stress terms are evaluated at $t^n$, whereas the pressure is evaluated at $t^{n+\theta_2}$. This is certainly permitted as the method may be shown to be fully consistent.

Using the auxiliary variables $\Delta U_i^\star$ and $\Delta U_i^{\star\star}$ we split Eq. (3.21) into two parts.

In the first form we remove all the pressure gradient terms from Eq. (3.21); in the second we retain in that equation the pressure gradient corresponding to the beginning of the step, i.e., $\partial p^n/\partial x_i$. Though it appears that the second split might be more accurate, there are other reasons for the success of the first split which we shall refer to later. Indeed Split A is the one which we shall universally recommend for steady-state problems. For transient problems however Split B with additional pressure stability or Split A with dual time stepping may give a slightly better result [83,87,93].

*Split A*

In this form we introduce an auxiliary variable $\Delta U_i^\star$ such that (removing third-order terms)

$$\Delta U_i^\star = \Delta t \left[ -\frac{\partial}{\partial x_j}(u_j U_i) + \frac{\partial \tau_{ij}}{\partial x_j} + \rho g_i + \frac{\Delta t}{2} u_k \frac{\partial}{\partial x_k}\left( \frac{\partial}{\partial x_j}(u_j U_i) - \rho g_i \right) \right]^n \tag{3.25}$$

We note that this equation is solved by an explicit time step applied to the discretized form and a complete solution is now possible. The "correction" given below is available once the pressure increment is evaluated:

$$\Delta U_i^{\star\star} = -\Delta t \frac{\partial p^{n+\theta_2}}{\partial x_i} + \frac{\Delta t^2}{2} u_k \frac{\partial^2 p^n}{\partial x_k \partial x_i} \tag{3.26}$$

From Eq. (3.1) we have

$$\Delta \rho = -\Delta t \frac{\partial U_i^{n+\theta_1}}{\partial x_i} = -\Delta t \left[ \frac{\partial U_i^n}{\partial x_i} + \theta_1 \frac{\partial \Delta U_i}{\partial x_i} \right] \tag{3.27}$$

Replacing $\Delta U_i$ by the known intermediate, auxiliary variable $\Delta U_i^\star$, using Eqs. (3.20) and (3.26) and rearranging and neglecting third- and higher-order terms we obtain

$$\Delta \rho = -\Delta t \left[ \frac{\partial U_i^n}{\partial x_i} + \theta_1 \frac{\partial \Delta U_i^\star}{\partial x_i} - \Delta t \theta_1 \left( \frac{\partial^2 p^n}{\partial x_i \partial x_i} + \theta_2 \frac{\partial^2 \Delta p}{\partial x_i \partial x_i} \right) \right] \tag{3.28}$$

The above equation is fully self-adjoint in the variable $\Delta\rho$ which is the unknown. Now, therefore, a standard Galerkin-type procedure can be optimally used for spatial

approximation of Eq. (3.28). It is clear that the governing equations can be solved after spatial discretization in the following order:

**(a)** Eq. (3.25) to obtain $\Delta U_i^\star$
**(b)** Eq. (3.28) to obtain $\Delta\rho$
**(c)** Eq. (3.26) to obtain $\Delta U_i^{\star\star}$ thus establishing the values of $U_i$ and $p$ from the energy and gas law at $t^{n+1}$

After completing the calculation to establish $\Delta U_i$ and $\Delta\rho$ the energy equation is dealt with independently and the value of $(\rho E)^{n+1}$ is obtained by the characteristic-Galerkin process applied to Eq. (3.7).

It is important to remark that this sequence allows us to solve the governing equations (3.1), (3.6), and (3.7) in an efficient manner and with adequate convection stabilization. Note that these equations are written in conservation form. Therefore, this algorithm is well suited for dealing with supersonic and hypersonic problems, in which the conservation form ensures that shocks will be placed at the right position and a unique solution achieved. However, we must remark that near the actual shocks, additional numerical damping will always be needed.

*Split B*

In this split we also introduce an auxiliary variable $\Delta U_i^\star$ now retaining the known values of $\partial p^n/\partial x_i$, i.e.,

$$\Delta U_i^\star = \Delta t\left[-\frac{\partial}{\partial x_j}(u_j U_i) + \frac{\partial \tau_{ij}}{\partial x_j} - \frac{\partial p}{\partial x_i} + \rho g_i + \frac{\Delta t}{2} u_k \frac{\partial}{\partial x_k}\left(\frac{\partial}{\partial x_j}(u_j U_i) + \frac{\partial p}{\partial x_i} - \rho g_i\right)\right]^n \tag{3.29}$$

It would appear that now $U_i^\star$ is a better approximation than that from Split A in (3.25).

We can now write the correction as

$$\Delta U_i^{\star\star} = -\theta_2 \Delta t \frac{\partial \Delta p}{\partial x_i} \tag{3.30}$$

i.e., the correction to be applied is smaller than that assuming Split A, Eq. (3.26). Further, if we use the fully explicit form with $\theta_2 = 0$, no mass velocity ($\Delta U_i^{\star\star}$) correction is necessary. We proceed to calculate the density changes as in Split A:

$$\Delta\rho = -\Delta t\left[\frac{\partial U_i^n}{\partial x_i} + \theta_1 \frac{\partial \Delta U_i^\star}{\partial x_i} - \Delta t \theta_1 \theta_2 \frac{\partial^2 \Delta p}{\partial x_i^2}\right] \tag{3.31}$$

The solution stages follow the same steps as in Split A. Later we will see that Split B does not possess the self-pressure stabilizing properties of Split A when incompressibility (or near incompressibility) is encountered (Section 3.6).

### 3.3.3 Spatial discretization and solution procedure

In all of the equations given below the standard Galerkin procedure is used for spatial discretization as this was fully justified for the characteristic-Galerkin method in Chapter 2. We now approximate spatially using standard finite element shape functions as

$$\begin{array}{llll} U_i = \mathbf{N}_u \tilde{\mathbf{U}}_i & \Delta U_i = \mathbf{N}_u \Delta \tilde{\mathbf{U}}_i & \Delta U_i^\star = \mathbf{N}_u \Delta \tilde{\mathbf{U}}_i^\star & \Delta U_i^{\star\star} = \mathbf{N}_u \Delta \tilde{\mathbf{U}}_i^{\star\star} \\ u_i = \mathbf{N}_u \tilde{\mathbf{u}}_i & p = \mathbf{N}_p \tilde{\mathbf{p}} & \rho = \mathbf{N}_\rho \tilde{\boldsymbol{\rho}} & \end{array} \tag{3.32}$$

In the above equation

$$\begin{aligned} \tilde{\mathbf{U}}_i &= \begin{bmatrix} U_i^1 & U_i^2 & \cdots & U_i^a & \cdots & U_i^m \end{bmatrix}^{\mathrm{T}} \\ \mathbf{N} &= \begin{bmatrix} N^1 & N^2 & \cdots & N^a & \cdots & N^m \end{bmatrix} \end{aligned} \tag{3.33}$$

where $a$ is the node (or variable) identifying number (and varies between 1 and $m$).

*Split A*

We have the following weak form of Eq. (3.25) for the standard Galerkin approximation (weighting functions are the shape functions):

$$\begin{aligned} &\int_\Omega N_u^a \Delta U_i^\star \, \mathrm{d}\Omega \\ &\quad = -\Delta t \left[ \int_\Omega N_u^a \frac{\partial}{\partial x_j} (u_j U_i) \, \mathrm{d}\Omega + \int_\Omega \frac{\partial N_u^a}{\partial x_j} \tau_{ij} \, \mathrm{d}\Omega - \int_\Omega N_u^a (\rho g_i) \, \mathrm{d}\Omega \right]^n \\ &\qquad + \frac{\Delta t^2}{2} \left[ \int_\Omega \frac{\partial}{\partial x_k} (u_k N_u^a) \left( -\frac{\partial}{\partial x_j} (u_j U_i) + \rho g_i \right) \mathrm{d}\Omega \right]^n \\ &\qquad + \Delta t \left[ \int_\Gamma N_u^a \tau_{ij} n_j \, \mathrm{d}\Gamma \right]^n \end{aligned} \tag{3.34}$$

Here, the viscous and stabilizing terms are integrated by parts and the last term is the boundary integral arising from integrating by parts the viscous contribution. Since the residual on the boundaries can be neglected, other boundary contributions from the stabilizing terms are negligible. Note from Eq. (2.105) that the whole residual appears in the stabilizing term. However, we have omitted diffusion terms in the above equation since they are of higher order.

As mentioned in Chapter 1, it is convenient to use matrix notation when the finite element formulation is carried out. We start here from Eq. (1.6) of Chapter 1 and repeat the deviatoric stress and strain rate relations below:

$$\tau_{ij} = 2\mu \left( \dot{\varepsilon}_{ij} - \tfrac{1}{3} \delta_{ij} \dot{\varepsilon}_{kk} \right) \tag{3.35}$$

where the quantity in brackets is the deviatoric strain rate. In the above

$$\dot{\varepsilon}_{ij} = \tfrac{1}{2} \left( \frac{\partial u_i}{\partial x_j} + \frac{\partial u_j}{\partial x_i} \right) \tag{3.36}$$

and

$$\dot{\varepsilon}_{kk} = \frac{\partial u_k}{\partial x_k} \tag{3.37}$$

We now define the strain rate in three dimensions by a six-component vector as given below:[1]

$$\dot{\boldsymbol{\varepsilon}} = \begin{bmatrix} \dot{\varepsilon}_{11} & \dot{\varepsilon}_{22} & \dot{\varepsilon}_{33} & 2\dot{\varepsilon}_{12} & 2\dot{\varepsilon}_{23} & 2\dot{\varepsilon}_{31} \end{bmatrix}^{\mathrm{T}} \tag{3.38}$$

With a matrix $\mathbf{m}$ defined as

$$\mathbf{m} = \begin{bmatrix} 1 & 1 & 1 & 0 & 0 & 0 \end{bmatrix}^{\mathrm{T}} \tag{3.39}$$

we find that the volumetric strain rate is

$$\dot{\varepsilon}_v = \dot{\varepsilon}_{ii} = \dot{\varepsilon}_{11} + \dot{\varepsilon}_{22} + \dot{\varepsilon}_{33} = \mathbf{m}^{\mathrm{T}} \dot{\boldsymbol{\varepsilon}} \tag{3.40}$$

The deviatoric strain rate can now be written simply as [see Eq. (3.33)]

$$\dot{\boldsymbol{\varepsilon}}^d = \dot{\boldsymbol{\varepsilon}} - \tfrac{1}{3}\mathbf{m}\dot{\varepsilon}_v = \left(\mathbf{I} - \tfrac{1}{3}\mathbf{m}\mathbf{m}^{\mathrm{T}}\right)\dot{\boldsymbol{\varepsilon}} = \mathbf{I}_d \dot{\boldsymbol{\varepsilon}} \tag{3.41}$$

where

$$\mathbf{I}_d = \left(\mathbf{I} - \tfrac{1}{3}\mathbf{m}\mathbf{m}^{\mathrm{T}}\right) \tag{3.42}$$

and thus

$$\mathbf{I}_d = \tfrac{1}{3}\begin{bmatrix} 2 & -1 & -1 & 0 & 0 & 0 \\ -1 & 2 & -1 & 0 & 0 & 0 \\ -1 & -1 & 2 & 0 & 0 & 0 \\ 0 & 0 & 0 & 3 & 0 & 0 \\ 0 & 0 & 0 & 0 & 3 & 0 \\ 0 & 0 & 0 & 0 & 0 & 3 \end{bmatrix} \tag{3.43}$$

The stresses are similarly written in vector form as

$$\boldsymbol{\sigma} = \begin{bmatrix} \sigma_{11} & \sigma_{22} & \sigma_{33} & \sigma_{12} & \sigma_{23} & \sigma_{31} \end{bmatrix}^{\mathrm{T}} \tag{3.44}$$

where of course $\sigma_{11}$ is equal to $\tau_{11} - p$ while $\sigma_{12}$ is identical to $\tau_{12}$, etc.

Immediately we can assume that the deviatoric stresses are proportional to the deviatoric strain rates and write directly from Eq. (3.35)

$$\boldsymbol{\sigma}^d = \mathbf{I}_d \boldsymbol{\sigma} = \mu \mathbf{I}_0 \dot{\boldsymbol{\varepsilon}}^d = \mu\left(\mathbf{I}_0 - \tfrac{2}{3}\mathbf{m}\mathbf{m}^{\mathrm{T}}\right)\dot{\boldsymbol{\varepsilon}} \tag{3.45}$$

where the diagonal matrix $\mathbf{I}_0$ is

$$\mathbf{I}_0 = \begin{bmatrix} 2 & & & & & \\ & 2 & & & & \\ & & 2 & & & \\ & & & 1 & & \\ & & & & 1 & \\ & & & & & 1 \end{bmatrix} \tag{3.46}$$

[1] In two dimensions we use a three-component vector $\dot{\boldsymbol{\varepsilon}} = \begin{bmatrix} \dot{\varepsilon}_{11} & \dot{\varepsilon}_{22} & 2\dot{\varepsilon}_{12} \end{bmatrix}^T$, noting that $\dot{\varepsilon}_{33}$ is zero.

To complete the matrix derivation the velocities and strain rates have to be appropriately related and the reader can verify that using the tensorial strain definitions we can write

$$\dot{\boldsymbol{\varepsilon}} = \mathcal{S}\mathbf{u} \tag{3.47}$$

where

$$\mathbf{u} = \begin{bmatrix} u_1 & u_2 & u_3 \end{bmatrix}^{\mathrm{T}} \tag{3.48}$$

and $\mathcal{S}$ is an appropriate strain rate matrix (operator) defined below:

$$\mathcal{S} = \begin{bmatrix} \dfrac{\partial}{\partial x_1} & 0 & 0 \\ 0 & \dfrac{\partial}{\partial x_2} & 0 \\ 0 & 0 & \dfrac{\partial}{\partial x_3} \\ \dfrac{\partial}{\partial x_2} & \dfrac{\partial}{\partial x_1} & 0 \\ 0 & \dfrac{\partial}{\partial x_3} & \dfrac{\partial}{\partial x_2} \\ \dfrac{\partial}{\partial x_3} & 0 & \dfrac{\partial}{\partial x_1} \end{bmatrix} \tag{3.49}$$

Finally the reader will note that the direct link between the strain rates and velocities will involve a matrix $\mathbf{B}$ defined simply by

$$\mathbf{B} = \mathcal{S}\mathbf{N}_u \tag{3.50}$$

Now from Eqs. (3.32), (3.34), and (3.45), the solution for $\Delta U_i^{\star}$ in matrix form is

*Step 1*

$$\Delta\tilde{\mathbf{U}}^{\star} = -\mathbf{M}_u^{-1}\Delta t\left[(\mathbf{C}_u\tilde{\mathbf{U}} + \mathbf{K}_\tau\tilde{\mathbf{u}} - \mathbf{f}) - \Delta t(\mathbf{K}_u\tilde{\mathbf{U}} + \mathbf{f}_s)\right]^n \tag{3.51}$$

where the quantities with a ˜ indicate nodal values and all the discretization matrices are similar to those defined in Chapter 2 for convection-diffusion equations (Eqs. 2.108 and 2.109) and are given as

$$\begin{aligned} \mathbf{M}_u &= \textstyle\int_\Omega \mathbf{N}_u^{\mathrm{T}}\mathbf{N}_u\,\mathrm{d}\Omega & \mathbf{C}_u &= \textstyle\int_\Omega \mathbf{N}_u^{\mathrm{T}}(\boldsymbol{\nabla}(\mathbf{u}\mathbf{N}_u))\,\mathrm{d}\Omega \\ \mathbf{K}_\tau &= \textstyle\int_\Omega \mathbf{B}^{\mathrm{T}}\mu\left(\mathbf{I}_0 - \tfrac{2}{3}\mathbf{m}\mathbf{m}^{\mathrm{T}}\right)\mathbf{B}\,\mathrm{d}\Omega & \mathbf{f} &= \textstyle\int_\Omega \mathbf{N}_u^{\mathrm{T}}\rho\mathbf{g}\,\mathrm{d}\Omega + \int_\Gamma \mathbf{N}_u^{\mathrm{T}}\mathbf{t}^d\,\mathrm{d}\Gamma \end{aligned} \tag{3.52}$$

where $\mathbf{g}$ is $[g_1\ g_2\ g_3]^{\mathrm{T}}$ and $\mathbf{t}^d$ is the traction corresponding to the deviatoric stress components.

In Eq. (3.51) $\mathbf{K}_u$ and $\mathbf{f}_s$ come from the terms introduced by the discretization along the characteristics. After integration by parts [i.e., from (3.34)], the expressions for $\mathbf{K}_u$ and $\mathbf{f}_s$ are

$$\mathbf{K}_u = -\tfrac{1}{2}\int_\Omega [\boldsymbol{\nabla}^{\mathrm{T}}(\mathbf{u}\mathbf{N}_u)]^{\mathrm{T}}[\boldsymbol{\nabla}^{\mathrm{T}}(\mathbf{u}\mathbf{N}_u)]\,\mathrm{d}\Omega \tag{3.53}$$

and

$$\mathbf{f}_s = -\tfrac{1}{2}\int_\Omega [\nabla^{\mathrm{T}}(\mathbf{u}\mathbf{N}_u)]^{\mathrm{T}}\rho\mathbf{g}\,\mathrm{d}\Omega \tag{3.54}$$

where $\nabla^T = [\partial/\partial x_1, \partial/\partial x_2, \partial/\partial x_3]$.

The weak form of the density-pressure equation is

$$\begin{aligned}\int_\Omega N_p^a \Delta\rho\,\mathrm{d}\Omega &= -\Delta t\int_\Omega N_p^a \frac{\partial}{\partial x_i}\left(U_i^n + \theta_1\Delta U_i^\star - \theta_1\Delta t\frac{\partial p^{n+\theta_2}}{\partial x_i}\right)\mathrm{d}\Omega \\ &= \Delta t\int_\Omega \frac{\partial N_p^a}{\partial x_i}\left[U_i^n + \theta_1\left(\Delta U_i^\star - \Delta t\frac{\partial p^{n+\theta_2}}{\partial x_i}\right)\right]\mathrm{d}\Omega \\ &\quad -\Delta t\int_\Gamma N_p^a\left[U_i^n + \theta_1\left(\Delta U_i^\star - \Delta t\frac{\partial p^{n+\theta_2}}{\partial x_i}\right)\right]n_i\mathrm{d}\Gamma\end{aligned} \tag{3.55}$$

In the above, all the RHS terms are integrated by parts. Further we shall discretize $\rho$ directly only in problems of compressible gas flows and therefore below we retain $p$ as the main variable. Spatial discretization of the above equation gives

*Step 2*

$$(\mathbf{M}_p + \Delta t^2\theta_1\theta_2\mathbf{H})\Delta\tilde{\mathbf{p}} = \Delta t[\mathbf{G}\tilde{\mathbf{U}}^n + \theta_1\mathbf{G}\Delta\tilde{\mathbf{U}}^\star - \Delta t\theta_1\mathbf{H}\tilde{\mathbf{p}}^n - \mathbf{f}_p] \tag{3.56}$$

which can be solved for $\Delta\tilde{\mathbf{p}}$.

The new matrices arising here are

$$\begin{aligned}&\mathbf{H} = \textstyle\int_\Omega(\nabla\mathbf{N}_p)^{\mathrm{T}}\nabla\mathbf{N}_p\,\mathrm{d}\Omega \quad \mathbf{M}_p = \int_\Omega \mathbf{N}_p^{\mathrm{T}}\left(\frac{1}{c^2}\right)^n\mathbf{N}_p\,\mathrm{d}\Omega \\ &\mathbf{G} = \textstyle\int_\Omega(\nabla\mathbf{N}_p)^{\mathrm{T}}\mathbf{N}_u\,\mathrm{d}\Omega \qquad \mathbf{f}_p = \Delta t\int_\Gamma \mathbf{N}_p^{\mathrm{T}}\mathbf{n}^{\mathrm{T}}[\tilde{\mathbf{U}}^n + \theta_1(\Delta\tilde{\mathbf{U}}^\star - \Delta t\nabla p^{n+\theta_2})]\,\mathrm{d}\Gamma\end{aligned} \tag{3.57}$$

In the above $\mathbf{f}_p$ contains boundary conditions as shown. We shall discuss these forcing terms fully in a later section as this form is vital to the success of the solution process. The weak form of the correction step from Eq. (3.26) is

$$\begin{aligned}\int_\Omega N_u^a\Delta U_i^{\star\star}\mathrm{d}\Omega &= \int_\Omega N_u^a\Delta U_i\,\mathrm{d}\Omega - \int_\Omega N_u^a\Delta U_i^\star\,\mathrm{d}\Omega \\ &= -\Delta t\int_\Omega N_u^a\left(\frac{\partial p^n}{\partial x_i} + \theta_2\frac{\partial\Delta p}{\partial x_i}\right)\mathrm{d}\Omega \\ &\quad -\frac{\Delta t^2}{2}\int_\Omega\frac{\partial}{\partial x_j}(u_j N_u^a)\frac{\partial p^n}{\partial x_i}\mathrm{d}\Omega\end{aligned} \tag{3.58}$$

The final stage of the computation of the mass flow vector $U_i^{n+1}$ is completed by the following matrix form:

*Step 3*

$$\Delta\mathbf{U}^{\star\star} = \Delta\tilde{\mathbf{U}} - \Delta\tilde{\mathbf{U}}^\star = -\mathbf{M}_u^{-1}\Delta t\left[\mathbf{G}^{\mathrm{T}}(\tilde{\mathbf{p}}^n + \theta_2\Delta\tilde{\mathbf{p}}) + \frac{\Delta t}{2}\mathbf{P}\tilde{\mathbf{p}}^n\right] \tag{3.59}$$

where

$$\mathbf{P} = \int_\Omega (\nabla(\mathbf{u}\mathbf{N}_u))^{\mathrm{T}} \nabla \mathbf{N}_p \, \mathrm{d}\Omega \tag{3.60}$$

At the completion of this stage the values of $\tilde{\mathbf{U}}^{n+1}$ and $\tilde{\mathbf{p}}^{n+1}$ are fully determined but the computation of the energy $(\rho E)^{n+1}$ is needed for gas flow problems so that pressure and density can be related through temperature.

Once again the energy equation (3.7) is identical in form to that of the scalar problem of convection-diffusion if we observe that $p$, $U_i$, etc., are known. The weak form of the energy equation is written using the characteristic-Galerkin approximation of Eq. (2.105) as

$$\begin{aligned}
&\int_\Omega N_E^k \Delta(\rho E)^{n+1} \, \mathrm{d}\Omega \\
&\quad = \Delta t \left[ -\int_\Omega N_E^k \frac{\partial}{\partial x_i}(u_i(\rho E + p)) \, \mathrm{d}\Omega - \int_\Omega \frac{\partial N_E^k}{\partial x_i} \left( \tau_{ij} u_j + k \frac{\partial T}{\partial x_i} \right) \mathrm{d}\Omega \right]^n \\
&\qquad + \frac{\Delta t^2}{2} \left[ \int_\Omega \frac{\partial}{\partial x_j}\left(u_j N_E^k\right) \left[ \frac{\partial}{\partial x_i}\left(-u_i\left(\rho E + p\right)\right) \right] \mathrm{d}\Omega \right]^n \\
&\qquad + \Delta t \left[ \int_\Gamma N_E^k \left( \tau_{ij} u_j + k \frac{\partial T}{\partial x_i} \right) n_i \, \mathrm{d}\Gamma \right]^n
\end{aligned} \tag{3.61}$$

*Step 4*

With the additional approximations

$$\rho E = \mathbf{N}_E \tilde{\mathbf{E}} \quad \text{and} \quad T = \mathbf{N}_T \tilde{\mathbf{T}} \tag{3.62}$$

we have

$$\Delta \tilde{\mathbf{E}} = -\mathbf{M}_E^{-1} \Delta t \left[ \mathbf{C}_E \tilde{\mathbf{E}} + \mathbf{C}_p \tilde{\mathbf{p}} + \mathbf{K}_T \tilde{\mathbf{T}} + \mathbf{K}_{\tau E} \tilde{\mathbf{u}} + \mathbf{f}_e - \Delta t (\mathbf{K}_{uE} \tilde{\mathbf{E}} + \mathbf{K}_{up} \tilde{\mathbf{p}} + \mathbf{f}_{es}) \right]^n \tag{3.63}$$

where $\tilde{\mathbf{E}}$ contains the nodal values of $\rho E$ and again the matrices and forcing vectors are similar to those previously obtained and given as

$$\begin{aligned}
\mathbf{M}_E &= \int_\Omega \mathbf{N}_E^{\mathrm{T}} \mathbf{N}_E \, \mathrm{d}\Omega \qquad \mathbf{C}_E = \int_\Omega \mathbf{N}_E^{\mathrm{T}} \nabla^{\mathrm{T}} (\mathbf{u}\mathbf{N}_E) \, \mathrm{d}\Omega \qquad \mathbf{C}_p = \int_\Omega \mathbf{N}_E^{\mathrm{T}} \nabla^{\mathrm{T}} (\mathbf{u}\mathbf{N}_p) \, \mathrm{d}\Omega \\
\mathbf{K}_T &= \int_\Omega (\nabla \mathbf{N}_E)^{\mathrm{T}} k \nabla \mathbf{N}_T \, \mathrm{d}\Omega \qquad \mathbf{K}_{\tau E} = \int_\Omega \mathbf{B}^{\mathrm{T}} \mu \mathbf{u}_{av} \left( \mathbf{I}_0 - \tfrac{2}{3} \mathbf{m}\mathbf{m}^{\mathrm{T}} \right) \mathbf{B} \, \mathrm{d}\Omega \\
\mathbf{K}_{uE} &= -\tfrac{1}{2} \int_\Omega (\nabla^{\mathrm{T}} (\mathbf{u}\mathbf{N}_E))^{\mathrm{T}} (\nabla \mathbf{N}_E) \, \mathrm{d}\Omega \qquad \mathbf{f}_e = \int_\Gamma \mathbf{N}_E^{\mathrm{T}} \mathbf{n}^{\mathrm{T}} (\mathbf{t}^d \mathbf{u} + k \nabla T) \, \mathrm{d}\Gamma \\
\mathbf{K}_{up} &= -\tfrac{1}{2} \int_\Omega (\nabla^{\mathrm{T}} (\mathbf{u}\mathbf{N}_E))^{\mathrm{T}} (\nabla \mathbf{N}_p) \, \mathrm{d}\Omega
\end{aligned} \tag{3.64}$$

The forcing term $\mathbf{f}_{es}$ contains source terms. For a three dimensional flow problem $\tau = \begin{bmatrix} \tau_{11} & \tau_{12} & \tau_{13} \\ \tau_{21} & \tau_{22} & \tau_{23} \\ \tau_{31} & \tau_{32} & \tau_{33} \end{bmatrix}$, if no source terms are available this term is equal to zero.

It is of interest to observe that the process of Step 4 can be extended to include in an identical manner the equations describing the transport of quantities such as turbulence parameters [43], chemical concentrations, etc., once the essential Steps 1–3 have been completed.

For isothermal compressible flows the first three steps of the CBS scheme are sufficient. However, for incompressible flows all four steps are required and the pressure should be related to density and temperature (energy) via a gas law (for example, the ideal gas law presented in this chapter).

*Split B*

With Split B, the discretization and solution procedures have to be modified slightly. Leaving the details of the derivation to the reader and using identical discretization processes, the final steps can be summarized as follows:

*Step 1*

$$\Delta\tilde{\mathbf{U}}_i^{\star} = -\mathbf{M}_u{}^{-1}\Delta t\left[(\mathbf{C}_u\tilde{\mathbf{U}} + \mathbf{K}_\tau\tilde{\mathbf{u}} + \mathbf{G}^{\mathrm{T}}\tilde{\mathbf{p}} - \mathbf{f}) - \Delta t\left(\mathbf{K}_u\tilde{\mathbf{U}} + \mathbf{f}_s + \frac{\Delta t}{2}\mathbf{P}\tilde{\mathbf{p}}\right)\right]^n \tag{3.65}$$

where all matrices are the same as in Split A except the forcing term $\mathbf{f}$ which is

$$\mathbf{f} = \int_\Omega \mathbf{N}_u^{\mathrm{T}}\rho\mathbf{g}\,\mathrm{d}\Omega + \int_\Gamma \mathbf{N}_u^{\mathrm{T}}\bar{\mathbf{t}}\,\mathrm{d}\Gamma \tag{3.66}$$

since the pressure term has now been integrated by parts.

*Step 2*

$$(\mathbf{M}_p + \Delta t^2\theta_1\theta_2\mathbf{H})\Delta\tilde{\mathbf{p}} = \Delta t[\mathbf{G}\tilde{\mathbf{U}}^n + \theta_1\mathbf{G}\Delta\tilde{\mathbf{U}}^{\star} - \mathbf{f}_p]^n \tag{3.67}$$

and

*Step 3*

$$\Delta\tilde{\mathbf{U}}^{\star\star} = -\mathbf{M}_u^{-1}\Delta t\left[\theta_2\mathbf{G}^{\mathrm{T}}\Delta\tilde{\mathbf{p}}\right] \tag{3.68}$$

Step 4, calculation of the energy, is unchanged. The reader can notice the differences in the above equations from those of Split A.

### 3.3.4 Mass diagonalization (lumping)

In Steps 1 to 3 of the split algorithm the solution often only requires the inversion (or solution) of mass matrices $\mathbf{M}_u$ and $\mathbf{M}_p$. Such steps are called explicit and generally are accomplished using approximation by a diagonal (lumped) form. Procedures for such diagonalization are described in Ref. [1]. Here we quote one which is generally efficient. In this the matrix form $\mathbf{M}_u$ is replaced by $\mathbf{M}^L$ computed as

$$M_{ab}^L = \delta_{ab}\int_\Omega N_a\,\mathrm{d}\Omega \qquad \text{no sum}$$

which the reader will recognize as the *row sum* of the full (consistent) mass matrix.

Such lumping for steady-state problems makes Steps 1 to 3 trivial and the errors involved are of no consequence as terms involving time variation disappear at a converged (steady-state) solution. However, for transient problems, quite serious errors can occur and in such cases an additional iteration is used to obtain a consistent solution. This already was discussed for the scalar equation in Section 2.6.3 [viz. Eq. (2.118)].

## 3.4 Explicit, semi-implicit, and nearly implicit forms

The split algorithm A or B will contain an explicit portion in the first characteristic-Galerkin step. However the second step, i.e., that of the determination of the pressure increment, can be made either explicit or implicit depending on the choice of $\theta_2$ and speed of sound. Now different stability criteria will apply ($\theta_1$ will always be taken to satisfy $1/2 \leq \theta_1 \leq 1$ and, thus, stability does not depend on it). We refer to schemes as being fully explicit or semi-implicit depending on the choice of the parameter $\theta_2$ as zero or nonzero, respectively. It is necessary at this point to mention that the fully explicit form is possible only for compressible flows for which $c \neq \infty$; however, later we will show that this restriction may be removed by introducing an "artificial compressibility."

It is also possible to solve the first step in a partially implicit manner to avoid severe time step restrictions. Now the viscous term is the one for which an implicit solution is sought. We refer to such schemes as quasi- (nearly) implicit schemes.

### 3.4.1 Fully explicit form

In fully explicit forms, $\frac{1}{2} \leq \theta_1 \leq 1$ and $\theta_2 = 0$. In general the time step limitations explained for the convection-diffusion equations are applicable, i.e.,

$$\Delta t \leq \frac{h}{c + |\mathbf{u}|} \tag{3.69}$$

if the viscosity effects are negligible. In the above equation $h$ is the element size, assuming linear elements only and one-dimensional behavior. For two- and three-dimensional flow problems determination of the element size is difficult. We shall discuss some possibilities in Section 3.4.4.

This particular form is very successful in compressible flow computations and has been widely used by the authors for solving many complex problems (see Chapter 7). More recently the algorithm has also been successfully used in conjunction with artificial compressibility to solve many other flow situations, including those in which incompressibility is involved (see Chapter 4).

### 3.4.2 Semi-implicit form

In semi-implicit form the following values apply:

$$\frac{1}{2} \leq \theta_1 \leq 1 \qquad \text{and} \qquad \frac{1}{2} \leq \theta_2 \leq 1 \tag{3.70}$$

Again the CBS algorithm is conditionally stable. The permissible time step is governed by the critical step of the characteristic-Galerkin explicit relation solved in Step 1 of the algorithm. This is the standard convection-diffusion problem discussed in Chapter 2 and the same stability limits apply, i.e.,

$$\Delta t \leq \Delta t_u = \frac{h}{|\mathbf{u}|} \tag{3.71a}$$

and/or

$$\Delta t \leq \Delta t_v = \frac{h^2}{2\nu} \tag{3.71b}$$

where $\nu$ is the kinematic viscosity. A convenient form incorporating both limits can be written as

$$\Delta t = min(\Delta t_u, \Delta t_v) \tag{3.72}$$

The reader can verify that the above relation will give appropriate time step limits with and without the domination of viscosity.

For slightly compressible or incompressible problems in which $\mathbf{M}_p$ is small or zero, the semi-implicit form is efficient and it should be noted that the matrix $\mathbf{H}$ of Eqs. (3.56) and (3.67) does not vary during the computation process. Therefore $\mathbf{H}$ can be factored into its triangular parts once leading to an economical direct procedure.

The implicit equation is usually solved either by direct solvers or by iterative (conjugate gradient) methods.

### 3.4.3 Quasi- (nearly) implicit form

To overcome the severe time step restriction made by the diffusion terms (e.g., viscosity or thermal conductivity), these terms can be treated implicitly. This involves solving separately an implicit form connecting the viscous terms with $\Delta U_i^\star$. Here, at each step, simultaneous equations need to be solved and this procedure can be of great advantage in certain cases such as high-viscosity flows and low Mach number flows [16,18,26,48]. Now the only time step limitation is $\Delta t \leq h/|\mathbf{u}|$ which appears to be a very reasonable and physically meaningful restriction.

### 3.4.4 Evaluation of time step limits: Local and global time steps

Though they are defined in terms of element sizes the time step values are established. In Fig. 3.1 the manner in which the size of the element is easily established at nodes is shown. In such cases, as seen, the element size is not unique for each node. In the calculation, we shall specify, if the scheme is conditionally stable, the time step limit at each node by assigning the minimum value for such nodes calculated from all elements connected to that node. When a problem is being solved in true time then obviously the smallest time step of all nodal values has to be adopted for the solution. However, in many problems it is possible to use *local time stepping* if steady-state solution is the only interest. In such problems local "nodal" time step values are conveniently used.

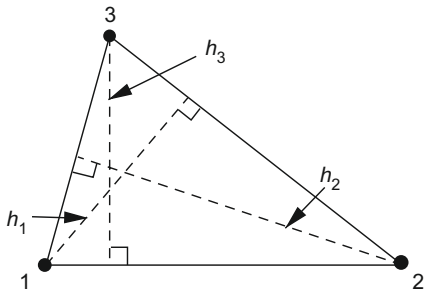


**FIGURE 3.1**
Element sizes at different nodes of a linear triangle.

This of course is equivalent to assuming identical time steps for the whole problem and simply adjusting the lumped masses. Such a problem with adjusted lumped masses is still physically and mathematically meaningful and we know that the convergence will be achieved as it invariably is. If only convective problems are considered, the time step needs only the element size in the direction of the streamline. This may very well be different from the minimum $h$. The procedure has been shown to be efficient by Thomas and Nithiarasu [94]. This is particularly important if the elements are elongated as we shall later mention in the case of supersonic flows with shocks.

Many steady-state problems have used such localized time stepping in the calculations.

In the context of local and global time stepping it is interesting to note that the stabilizing terms introduced by the characteristic-Galerkin process will not take on the optimal value for any element in which the time step differs from the critical one; that is of course if we use local time stepping we shall automatically achieve this optimal value often throughout all elements at least for steady-state problems. However, on other occasions it may be useful to make sure that (a) in all elements we introduce optimal damping and (b) that the progressive time step for all elements is identical. The latter of course is absolutely necessary if for instance we deal with transient problems where all time steps are real. For such cases it is possible to consider the $\Delta t$ as being introduced in two stages: (1) as the $\Delta t_{\text{ext}}$ which has of course to preserve stability and must be left at a minimum $\Delta t$ calculated from any element; and (2) to use in the calculation of each individual element the $\Delta t_{\text{int}}$ which is optimal for an element, as of course exceeding the stability limit does not matter there and we are simply adding better damping characteristics. Here the $\Delta t_{\text{int}}$ is the only one occurring in convection stabilizing terms.

This internal-external subdivision is of some importance when incompressibility effects are considered. As shown in the next section, the stabilizing diagonal term occurs in steady-state problems depending on the size of the time step. If the mesh is graded and very small elements dictate the time step over the whole domain, we might find that the diagonal term introduced overall is not sufficient to preserve

incompressibility. For such problems we recommend the use of internal and external time steps which differ and we introduced these in Ref. [53]. In this case the internal time step $\Delta t_{\text{int}}$ is the one multiplying the second-order pressure terms at Step 2.

## 3.5 Artificial compressibility and dual time stepping

### 3.5.1 Artificial compressibility for steady-state problems

When the real compressibility is small, it is often assumed that the fluid is incompressible with the speed of sound approaching infinity. Even if the speed of sound is finite, its value will have to be large and hence a very severe time step limitation arises. However, an artificial compressibility method can be employed to eliminate the restrictions posed by the speed of sound at Step 2 by taking an artificial value for the speed of sound which is sufficiently low. This of course only possible if steady-state conditions exist and therefore in that limit the transient term disappears. Step 2 of the CBS scheme may be rewritten in its semi-discrete form as [57]

$$\begin{aligned}\Delta\rho &= \left(\frac{1}{c^2}\right)^n \Delta p \approx \left(\frac{1}{\beta^2}\right)^n \Delta p \\ &= -\Delta t\left[\frac{\partial U_i^n}{\partial x_i} + \theta_1 \frac{\partial \Delta U_i^\star}{\partial x_i} - \Delta t\theta_1\left(\frac{\partial^2 p^n}{\partial x_i \partial x_i} + \theta_2 \frac{\partial^2 \Delta p}{\partial x_i \partial x_i}\right)\right]\end{aligned} \tag{3.73}$$

where $\beta$ is an artificial parameter with the dimensions of velocity. This parameter may be either given as a constant throughout the domain or determined based on the convective or diffusive time step restrictions. We recommend the latter option, as this results in manageable local and global time step sizes. The $\beta$ value may be locally computed using the following relation so that the convective and viscous time steps are represented:

$$\beta = max(\varepsilon, u_{conv}, u_{diff}) \tag{3.74}$$

where $\varepsilon$ is a small constant and it makes sure that the $\beta$ is not approaching zero under any circumstances. $u_{conv}$ and $u_{diff}$ are respectively the convection and diffusion velocities given as

$$\begin{aligned} u_{conv} &= |\mathbf{u}| = \sqrt{u_i u_i} \\ u_{diff} &= \frac{\nu}{h} \end{aligned} \tag{3.75}$$

where $h$ is the element size and $\nu$ is the kinematic viscosity.

The three steps of the CBS scheme follow exactly the procedure discussed in the preceding sections. However, the difference here is that no coupling exists between the energy and the rest of the governing equations. Note that the time step limitation for the artificial compressibility method may be written as

$$\Delta t = \frac{h}{|\mathbf{u}| + \beta} \tag{3.76}$$

The above relation includes the viscous effect via the artificial parameter. The artificial compressibility method explained here is valid for steady flows. However, an appropriate dual time-stepping method, explained in the following subsection, should be employed to recover a true transient solution.

### 3.5.2 Artificial compressibility in transient problems (dual time stepping)

A transient formulation for the artificial compressibility method is easy to derive within the CBS framework. Unlike standard artificial compressibility methods, the present formulation is stable for both convection and pressure effects [57,58]. The main difference between the CBS formulation presented before and the artificial compressibility formulation is that the time step $\Delta t$ here is treated as a pseudo iterative time step to reach an instantaneous steady state within a real time step $\Delta\tau$. This requires addition of a real time term to the semi-discrete form of the momentum equation, i.e., [from Eq. (3.21)],

$$\begin{aligned} U_i^{n+1} - U_i^n = \Delta t\Bigg[ &- \frac{\partial}{\partial x_j}(u_j U_i)^n + \frac{\partial \tau_{ij}^n}{\partial x_j} + (\rho g_i)^n - \frac{\Delta U_i^m}{\Delta \tau}\Bigg] - \Delta t \frac{\partial p^{n+\theta_2}}{\partial x_i} \\ &+ \frac{\Delta t^2}{2} u_k \frac{\partial}{\partial x_k}\Bigg[\frac{\partial}{\partial x_j}(u_j U_i) - \frac{\partial \tau_{ij}^n}{\partial x_j} - \rho g_i + \frac{\Delta U_i^m}{\Delta \tau}\Bigg]^n \\ &+ \frac{\Delta t^2}{2} u_k \frac{\partial}{\partial x_k}\left(\frac{\partial p^{n+\theta_2}}{\partial x_i}\right) \end{aligned} \tag{3.77}$$

where $\Delta U_i^m$ is the real time variation of the variable $U_i$. This term may be approximated depending on the transient accuracy requirement. The second-order accuracy may be obtained by approximating

$$\Delta U_i^m = \frac{3U_i^n - 4U_i^m + U_i^{m-1}}{2} \tag{3.78}$$

Here superscript $m$ refers to the real time variation. It is easy to understand from Eq. (3.77) that at pseudo-steady state $U_i^{n+1} = U_i^n$ and this leads to the recovery of the semi-discrete form of the momentum equation in real time. Incorporating the above changes into the CBS formulation, the three semi-discrete steps of the CBS scheme may be written for Split A as

$$\begin{aligned} \Delta U_i^\star = \Delta t\Bigg[ &- \frac{\partial}{\partial x_j}(u_j U_i) + \frac{\partial \tau_{ij}}{\partial x_j} + \rho g_i \\ &+ \frac{\Delta t}{2} u_k \frac{\partial}{\partial x_k}\left(\frac{\partial}{\partial x_j}(u_j U_i) - \frac{\partial \tau_{ij}}{\partial x_j} - \rho g_i\right)\Bigg]^n \end{aligned} \tag{3.79}$$

is the first step. We note that this equation is solved by an explicit time step. As before, the "correction" given below is available once the pressure increment is evaluated

(Step 3):

$$\Delta U_i^{\star\star} = \Delta U_i - \Delta U_i^{*} = -\Delta t \frac{\partial p^{n+\theta_2}}{\partial x_i} - \frac{\Delta U_i^m}{\Delta \tau} + \frac{\Delta t^2}{2} u_k \frac{\partial^2 p^n}{\partial x_k \partial x_i} + \frac{\Delta t^2}{2} u_k \frac{\partial}{\partial x_k}\left(\frac{\Delta U_i^m}{\Delta \tau}\right) \tag{3.80}$$

The modified form of Eq. (3.1) is now written as

$$\Delta \rho = \frac{1}{\beta^2}\Delta p = -\Delta t \frac{\partial U_i^{n+\theta_1}}{\partial x_i} = -\Delta t \left[\frac{\partial U_i^n}{\partial x_i} + \theta_1 \frac{\partial \Delta U_i}{\partial x_i}\right] \tag{3.81}$$

Replacing $\Delta U_i$ with $\Delta U_i^{*} + \Delta U_i^{**}$ and rearranging after neglecting third- and higher-order terms we obtain (final form of Step 2)

$$\frac{1}{\beta^2}\Delta p = -\Delta t \left[\frac{\partial U_i^n}{\partial x_i} + \theta_1 \frac{\partial \Delta U_i^{\star}}{\partial x_i} - \Delta t \theta_1 \left(\frac{\partial^2 p^n}{\partial x_i \partial x_i} + \theta_2 \frac{\partial^2 \Delta p}{\partial x_i \partial x_i}\right) - \theta_1 \frac{\partial}{\partial x_i}\left(\frac{\Delta U_i^m}{\Delta \tau}\right)\right] \tag{3.82}$$

The method described above brings together all three steps several times within a real time step $\Delta\tau$. This strongly couples the three steps within every real time step $\Delta\tau$ and produces a one-step monolithic type approximation. As a result, the splitting errors faced by standard fractional step methods do not apply here. To demonstrate this, all three steps should be considered at a pseudo steady state, i.e., when $\Delta U_i = 0$. Combining Steps 1 [Eq. (3.79)] and 3 [Eq. (3.80)] gives

$$-\left[\frac{\Delta U_i^m}{\Delta \tau} + \frac{\partial}{\partial x_j}(u_j U_i) + \frac{\partial p}{\partial x_i} - \frac{\partial \tau_{ij}}{\partial x_j} - (\rho g_i)\right]^n + \frac{\Delta t}{2} u_k \frac{\partial}{\partial x_k}\left[\frac{\partial}{\partial x_j}(u_j U_i) - \frac{\partial \tau_{ij}}{\partial x_j} - \rho g_i + \frac{\Delta U_i^m}{\Delta \tau} + \frac{\partial p}{\partial x_i}\right]^n = 0 \tag{3.83}$$

Substituting Step 1 [Eq. (3.79)] into Step 2 [Eq. (3.82)], neglecting third- and higher-order terms, and rearranging (assuming $\theta_1 = 0.5$, $\theta_2 = 0$ and pseudo steady state with $\triangle p = 0$)

$$\frac{\partial U_i^n}{\partial x_i} + \frac{\Delta t}{2}\frac{\partial}{\partial x_i}\left[\frac{\partial (u_j U_i)}{\partial x_j} - \frac{\partial \tau_{ij}}{\partial x_j} - \rho g + \frac{\partial p}{\partial x_i} + \frac{\Delta U_i^m}{\Delta \tau}\right]^n = 0 \tag{3.84}$$

Equations (3.83) and (3.84) clearly show that the equations are consistent. As shown the conservation of momentum and conservation of mass equations for incompressible flows in their semi-discrete form are recovered along with the convection and pressure stabilization terms. It is also obvious from these equations that the stabilization terms are functions of the residual and the stabilization coefficient is proportional to pseudo time step $\Delta t$. Since $n = m + 1$ at instantaneous steady state, this scheme is equivalent to a stabilized implicit monolithic method [87].

## 3.6 "Circumvention" of the Babuška-Brezzi (BB) restrictions

In the previous sections we have not restricted the nature of the interpolation functions for shape functions $\mathbf{N}_u$ and $\mathbf{N}_p$. If we choose these interpolations in a manner satisfying the mixed patch test conditions [1,95,96] or the Babuška-Brezzi (BB) restriction for incompressibility [2,3] (also see Chapter 4 for some permissible interpolations) then of course completely incompressible problems can be dealt with without any special difficulties by both Split A and Split B formulations. However Split A introduces an important bonus which permits us to avoid any restrictions on the nature of the two shape functions used for velocity and pressure. Let us examine here the structure of the equations obtained in steady-state conditions. For simplicity we shall consider here only the Stokes form of the governing equations in which the convective terms disappear. Further we shall take the fluid as incompressible (e.g., $c = \infty$) and thus uncoupled from the energy equations. Now the three steps of Split A given in Eqs. (3.51), (3.56), and (3.59) are written as

$$\begin{aligned}
\Delta\tilde{\mathbf{U}}^{\star} &= -\Delta t \mathbf{M}_u^{-1}[\mathbf{K}_\tau \tilde{\mathbf{u}}^n - \mathbf{f}] \\
\Delta\tilde{\mathbf{p}} &= \frac{1}{\Delta t \theta_1 \theta_2}\mathbf{H}^{-1}[\mathbf{G}\tilde{\mathbf{U}}^n + \theta_1 \mathbf{G}\Delta\tilde{\mathbf{U}}^{\star} - \Delta t \theta_1 \mathbf{H}\tilde{\mathbf{p}}^n - \mathbf{f}_p] \\
\Delta\tilde{\mathbf{U}}^{\star\star} &= \Delta\tilde{\mathbf{U}} - \Delta\tilde{\mathbf{U}}^{\star} = -\Delta t \mathbf{M}_u^{-1}\mathbf{G}^{\mathrm{T}}(\tilde{\mathbf{p}}^n + \theta_2 \Delta\tilde{\mathbf{p}})
\end{aligned} \tag{3.85}$$

At steady state we have $\Delta\tilde{\mathbf{p}} = \Delta\tilde{\mathbf{U}} = \mathbf{0}$ and eliminating $\Delta\tilde{\mathbf{U}}^{\star}$ and $\Delta\tilde{\mathbf{U}}^{\star\star}$ we can write (dropping now the superscript $n$) from the first and third of Eqs. (3.85)

$$\mathbf{K}_\tau \tilde{\mathbf{u}} + \mathbf{G}^{\mathrm{T}}\tilde{\mathbf{p}} = \mathbf{f} \tag{3.86}$$

and

$$\mathbf{G}\tilde{\mathbf{U}} + \theta_1 \Delta t \mathbf{G}\mathbf{M}_u^{-1}\mathbf{G}^{\mathrm{T}}\tilde{\mathbf{p}} - \Delta t \theta_1 \mathbf{H}\tilde{\mathbf{p}} - \mathbf{f}_p = 0 \tag{3.87}$$

from the second and third of Eqs. (3.85)

We finally have a system which can be written in the form

$$\begin{bmatrix} \mathbf{K}_\tau/\rho & \mathbf{G}^{\mathrm{T}} \\ \mathbf{G} & \Delta t \theta_1 \left[\mathbf{G}\mathbf{M}_u^{-1}\mathbf{G}^{\mathrm{T}} - \mathbf{H}\right] \end{bmatrix} \begin{Bmatrix} \tilde{\mathbf{U}} \\ \tilde{\mathbf{p}} \end{Bmatrix} = \begin{Bmatrix} \mathbf{f}_1 \\ \mathbf{f}_2 \end{Bmatrix} \tag{3.88}$$

Here $\mathbf{f}_1$ and $\mathbf{f}_2$ arise from the forcing terms.

The system is now always positive definite [41] and therefore leads to a non-singular solution for *any interpolation functions* $\mathbf{N}_u$, $\mathbf{N}_p$ chosen. In most of the examples discussed in this book and elsewhere equal interpolation is used for both the $U_i$ and $p$ variables, i.e., $\mathbf{N}_u = \mathbf{N}_p$. We must however stress that any other interpolation can be used without violating the stability. This is an important reason for the preferred use of the Split A form.

If the pressure gradient term is retained as in Eq. (3.29), (i.e., if we use Split B) the lower diagonal term of Eq. (3.88) is identically zero and the BB conditions in the

full scheme cannot be avoided. To show this we start from Eqs. (3.65), (3.67), and (3.68). For incompressible Stokes flow we have

$$\begin{aligned}\Delta\tilde{\mathbf{U}}_i^{\star} &= -\mathbf{M}_u^{-1}\Delta t\left[\mathbf{K}_\tau\tilde{u}+\mathbf{G}^{\mathrm{T}}\tilde{\mathbf{p}}-\mathbf{f})\right]^n\\ \Delta\tilde{\mathbf{p}} &= \frac{1}{\Delta t\theta_1\theta_2}\mathbf{H}^{-1}\Delta t\left[\mathbf{G}\tilde{\mathbf{U}}^n+\theta_1\mathbf{G}\Delta\tilde{\mathbf{U}}^{\star}-\mathbf{f}_p\right]\\ \Delta\tilde{\mathbf{U}}^{\star\star} &= -\mathbf{M}_u^{-1}\Delta t\left[\theta_2\mathbf{G}^{\mathrm{T}}\Delta\tilde{\mathbf{p}}\right]\end{aligned} \tag{3.89}$$

At steady state $\Delta\tilde{\mathbf{p}}=\Delta\tilde{\mathbf{U}}=\mathbf{0}$, which gives the following two equations:

$$\mathbf{K}_\tau\tilde{\mathbf{u}}+\mathbf{G}^{\mathrm{T}}\tilde{\mathbf{p}}=\mathbf{f} \tag{3.90}$$

and

$$\mathbf{G}\tilde{\mathbf{U}}=\mathbf{f}_p \tag{3.91}$$

Note that $\Delta\mathbf{U}_i^{\star\star}$ is zero from the third of Eq. (3.89). As in Split A we can write the following system:

$$\begin{bmatrix}\mathbf{K}_\tau/\rho & \mathbf{G}^{\mathrm{T}}\\ \mathbf{G} & \mathbf{0}\end{bmatrix}\begin{Bmatrix}\tilde{\mathbf{U}}\\ \tilde{\mathbf{p}}\end{Bmatrix}=\begin{Bmatrix}\mathbf{f}_1\\ \mathbf{f}_2\end{Bmatrix} \tag{3.92}$$

where $\mathbf{f}_1$ and $\mathbf{f}_2$ arise from the forcing terms as in the Split A form. Clearly here the BB restrictions are not circumvented.

It is interesting to observe that the lower diagonal term which appeared in Eq. (3.88) is equivalent to the difference between the so-called fourth-order and second-order finite difference approximations of the Laplacian. This justifies the use of similar terms introduced into the computation by Jameson and Mavripolis [97].

## 3.7 A single-step version

If the $\Delta\mathbf{U}_i^{\star}$ term in Eq. (3.28) is omitted, the intermediate variable $U_i^{\star}$ need not be determined. Instead we can directly calculate $\rho$ (or $p$), $U_i$, and $\rho E$. This of course introduces an additional approximation.

The approximation of Eq. (3.1) is not necessary in any expected fully explicit scheme as the density increment is directly obtained if we note that

$$\mathbf{M}_p\Delta\tilde{\mathbf{p}}=\mathbf{M}_u\Delta\tilde{\boldsymbol{\rho}} \tag{3.93}$$

With the above simplifications Split A becomes

$$\Delta\tilde{\boldsymbol{\Phi}}=-\mathbf{M}_u^{-1}\Delta t\left[\int_\Omega\mathbf{N}^{\mathrm{T}}\left(\frac{\partial\mathbf{F}_i}{\partial x_i}+\frac{\partial\mathbf{G}_i}{\partial x_i}\right)\mathrm{d}\Omega-\tfrac{1}{2}\Delta t\int_\Omega\mathbf{N}^{\mathrm{T}}\mathbf{D}\,\mathrm{d}\Omega\right]^n \tag{3.94}$$

omitting the source terms for clarity [$\mathbf{F}_i$ and $\mathbf{G}_i$ are explained in Chapter 1, Eqs. (1.26b) and (1.26c)] and noting that now $\tilde{\boldsymbol{\Phi}}$ denotes all the variables. The added stabilizing

terms $\mathbf{D}$ are defined below and have to be integrated by parts in the usual manner:

$$\begin{Bmatrix} 2\theta_1 \dfrac{\partial p^2}{\partial x_i \partial x_i} \\ u_i \dfrac{\partial}{\partial x_i}\left[\dfrac{\partial}{\partial x_j}(u_j \rho u_1) + \dfrac{\partial p}{\partial x_1}\right] \\ u_i \dfrac{\partial}{\partial x_i}\left[\dfrac{\partial}{\partial x_j}(u_j \rho u_2) + \dfrac{\partial p}{\partial x_2}\right] \\ u_i \dfrac{\partial}{\partial x_i}\left[\dfrac{\partial}{\partial x_j}(u_j \rho u_3) + \dfrac{\partial p}{\partial x_3}\right] \\ u_i \dfrac{\partial}{\partial x_i}\left[\dfrac{\partial}{\partial x_j}(u_j \rho E + u_j p)\right] \end{Bmatrix} \tag{3.95}$$

The added "diffusions" are simple and are streamline oriented, and thus do not mask the true effects of viscosity as it happens in some schemes (e.g., the Taylor-Galerkin process).

If only steady-state results are sought it would appear that $\Delta t$ multiplying the matrix $\mathbf{D}$ should be set at its optimal value of $\Delta t_{\text{crit}} \approx h/|\mathbf{u}|$ and we generally recommend, providing the viscosity is small, this value for the full scheme [37].

However the oversimplified scheme of Eq. (3.94) can lose some accuracy and even when steady state is reached it will give slightly different results than those obtained using the full sequential updating [37]. However at low Mach numbers the difference is negligible as we shall show later in Section 3.10. The small additional cost involved in computing the two-step sequence $\Delta\tilde{\mathbf{U}}^{\star} \rightarrow \Delta\mathbf{p} \rightarrow \Delta\tilde{\mathbf{U}} \rightarrow \Delta\tilde{\mathbf{E}}$ will have to be balanced against the accuracy increase. In general, we have found that the two-step version is preferable.

However it is interesting to consider once again the performance of the single-step scheme in the case of Stokes equations as we did for the other schemes in the previous section. After discretization we have, omitting convective terms, only one additional diffusion term which arises [Eq. (3.82)] in the mass conservation equation. After discretization, in steady state

$$\begin{bmatrix} \mathbf{K}_\tau/\rho & \mathbf{G}^{\mathrm{T}} \\ \mathbf{G} & \theta_1 \Delta t \mathbf{H} \end{bmatrix} \begin{Bmatrix} \tilde{\mathbf{U}} \\ \tilde{\mathbf{p}} \end{Bmatrix} = \begin{Bmatrix} \mathbf{f}_1 \\ \mathbf{f}_2 \end{Bmatrix} \tag{3.96}$$

Clearly the single-step algorithm retains the capacity of dealing with full incompressibility without stability problems but of course can only be used for the nearly incompressible range of problems for which $\mathbf{M}_p$ exists. We should remark here that this formulation now achieves precisely the same stabilization as that suggested by Brezzi and Pitkäranta [98], see Chapter 10 in Ref. [1].

We shall note the performance of single- and two-step algorithms in Section 3.10 of this chapter.

## 3.8 Splitting error

As shown previously the CBS algorithm with Split A provides conditional pressure stability and thus spurious pressure modes can be reduced. However, due to the three-step procedure introduced within the CBS procedure it is prone to a "so-called" splitting error. One such error is the first-order error temporal in pressure. This is a widely discussed topic in the literature with application to the quasi-implicit form of the CBS or similar splitting methods (often referred to as the semi-implicit fractional step method) [93,99–102]. This is mainly a topic in incompressible flows. In order to explain the splitting error, we need to first consider the pressure Poisson equation of Step 2. When using the quasi-implicit form of the algorithm, the pressure Poisson equation is reduced to [substitute $\Delta\rho = 0, \theta_1 = \theta_2 = 1$ into Eq. (3.28)]

$$\frac{\partial^2 p^{n+1}}{\partial x_i^2} = \frac{\rho}{\Delta t}\left(\frac{\partial u_i^*}{\partial x_i}\right) \tag{3.97}$$

However, if the momentum equation for incompressible flow is differentiated with respect to $x_i$ (divergence) and the incompressibility constrain is applied, we obtain

$$\frac{\partial^2 p}{\partial x_i^2} = -\rho\frac{\partial}{\partial x_i}\left(\frac{\partial(u_i u_j)}{\partial x_j}\right) \tag{3.98}$$

Since the discrete form of Eq. (3.97) and continuous form of Eq. (3.98) are equal only to first order in time, a first-order pressure error is introduced into the three-step split procedure. This error can be demonstrated by substituting the intermediate velocity field of the quasi-implicit form (without source)

$$\rho\Delta u_i^\star = \Delta t\Bigg[-\rho\frac{\partial}{\partial x_j}(u_j u_i) + \mu\frac{\partial^2 u_i^\star}{\partial x_j \partial x_j} + \frac{\delta t}{2}u_k\frac{\partial}{\partial x_k}\left(\rho\frac{\partial}{\partial x_j}(u_j u_i) - \mu\frac{\partial^2 u}{\partial x_j x_i}\right)^n\Bigg] \tag{3.99}$$

into Eq. (3.97). Substituting $u^\star = (u + \Delta t\partial p/\partial x_i)^{n+1}$ into the RHS of Eq. (3.99) (neglecting the stabilization terms for simplicity) gives

$$\rho u_i^* = \rho u_i^n - \Delta t\left[\rho\frac{\partial(u_i u_j)^n}{\partial x_j} - \mu\frac{\partial^2}{\partial x_j \partial x_j}\left(u + \Delta t\frac{\partial p}{\partial x_i}\right)^{n+1}\right] \tag{3.100}$$

Substituting Eq. (3.100) into Eq. (3.97) and applying conservation of mass and simplifying (note that $u^{n+1} = u^n + \Delta t\frac{\partial u}{\partial t}^n$), we obtain

$$\frac{\partial^2 p^{n+1}}{\partial x_i^2} = -\frac{\partial}{\partial x_i}\left[\rho\frac{\partial(u_i u_j)^n}{\partial x_j}\right] + \Delta t\mu\frac{\partial}{\partial x_i}\left[\frac{\partial^2}{\partial x_j \partial x_j}\left(\frac{\partial u}{\partial t}\right)^n\right] + \Delta t\mu\frac{\partial}{\partial x_i}\left[\frac{\partial^2}{\partial x_j \partial x_j}\left(\frac{\partial p}{\partial x_i}\right)^{n+1}\right] \tag{3.101}$$

Comparison of Eqs. (3.101) and (3.98) clearly shows that the discrete form of Eq. (3.97) leads to first-order error terms in time. Note that the second term on the RHS of the above equation is equal to zero for incompressible flows.

### 3.8.1 Elimination of first-order pressure error

One of the early methods proposed [99] to remove the first-order pressure error was to first calculate the approximate pressure $p_{old}$ from Eq. (3.97) and then use the correction

$$p_{new} = p_{old} - \mu \Delta t \frac{\partial^2 p_{old}}{\partial x_i^2} \tag{3.102}$$

This correction eliminates the last term in Eq. (3.101).

At low Reynolds numbers and for Stokes flow, adding dual time stepping to the CBS scheme is an alternative way of reducing the first-order pressure error. Adding dual time stepping as explained in Section 3.5.2 replaces the first-order pressure error with the following form at the instantaneous steady state ($\Delta u/\Delta t \approx 0$):

$$\begin{aligned}\frac{\partial^2 p^{n+1}}{\partial x_i^2} = &-\frac{1}{\Delta t}\frac{\partial}{\partial x_i}\left[\rho \Delta t \frac{\partial (u_i u_j)^n}{\partial x_j}\right] \\ &+ \Delta t \mu \frac{\partial}{\partial x_i}\left[\frac{\partial^2}{\partial x_j \partial x_j}\left(\frac{\partial p}{\partial x_i} + \frac{\Delta u^m}{\Delta \tau}\right)^{n+1}\right]\end{aligned} \tag{3.103}$$

Substituting for $\Delta u^m/\Delta\tau$ at instantaneous steady state from Section 3.5.2, we get

$$\begin{aligned}\frac{\partial^2 p^{n+1}}{\partial x_i^2} = &-\frac{1}{\Delta t}\frac{\partial}{\partial x_i}\left[\rho \Delta t \frac{\partial (u_i u_j)^n}{\partial x_j}\right] \\ &+ \Delta t \mu \frac{\partial}{\partial x_i}\left[\frac{\partial^2}{\partial x_j \partial x_j}\left(-\rho \frac{\partial u_i u_j}{\partial x_j} + \mu \frac{\partial^2 u_i}{\partial x_j \partial x_j}\right)^{m+1}\right]\end{aligned} \tag{3.104}$$

The error now is a function of $\Delta t$, the pseudo time step, not the real time step $\Delta\tau$.

## 3.9 Boundary conditions

### 3.9.1 Fictitious boundaries

In a large number of fluid mechanics problems the flow in open domains is considered. A typical open domain describing flow past an aircraft wing is shown in Fig. 3.2. In such problems the boundaries are simply limits of computation and they are therefore fictitious. With suitable values specified at such boundaries, however, accurate solution for the flow inside the isolated domain can be achieved.

Generally as the distance from the object grows, the boundary values tend to those encountered in the free domain flow or the flow at infinity. This is particularly true at

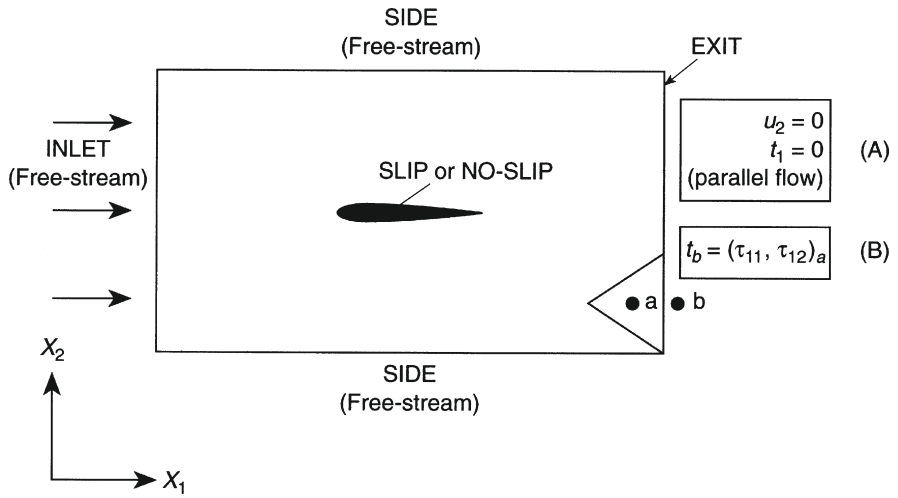


**FIGURE 3.2**
Fictitious and real boundaries.

the entry and side boundaries shown in Fig. 3.2. At the exit, however, the conditions are different and here the effect of the introduced disturbance can continue for a very large distance denoting the wake of the problem. We shall from time to time discuss problems of this nature but now we shall simply make the following remarks.

1. If the flow is subsonic the specification of all quantities except the density (or pressure) can be made on both the side and entry boundaries.
2. Whereas for supersonic flows all the variables can be prescribed at the inlet or side boundaries, at the exit boundary however no conditions can be imposed simply because by definition no disturbance in a supersonic stream can travel upstream.

With subsonic exit conditions the situation is somewhat more complex and here various possibilities exist. We again illustrate such conditions in Fig. 3.2.

*Condition A:* Denoting the most obvious assumptions with regard to the traction and velocities.
*Condition B:* A more sophisticated condition of zero gradient of traction and stresses existing there. Such conditions will of course always apply to the exit domains for incompressible flow. Condition B was first introduced by Zienkiewicz et al. [88] and is discussed fully by Papanastasiou et al. [103]. This condition is of some importance as it gives remarkably good answers.

We shall refer to these open boundary conditions in various classes of problems dealt with later in this book and shall discuss them in detail.

Of considerable importance, especially in view of the CBS scheme, are conditions which we will encounter on real boundaries.

### 3.9.2 Real boundaries

By real boundaries we mean limits of fluid domains which are physically defined and here three different possibilities exist.

1. *Solid boundaries with no-slip conditions*: On such boundaries the fluid is assumed to stick or attach itself to the boundary and thus all velocity components become zero. Obviously this condition is only possible for viscous flows.
2. *Solid boundaries in inviscid flow* (*slip conditions*): When the flow is inviscid we will always encounter slipping boundary conditions where only the normal velocity component is specified. This will generally be zero if the boundaries are stationary. Such boundary conditions will invariably be imposed for problems of Euler flow whether it is compressible or incompressible.
3. *Prescribed traction boundary conditions*: The last category is that of boundaries on which tractions are prescribed. This includes zero traction in the case of free surfaces of fluids or any prescribed tractions such as those caused by wind being imposed on the surface.

These three basic kinds of boundary conditions have to be imposed on the fluid and special consideration has to be given to these when split operator schemes are used.

### 3.9.3 Application of real boundary conditions in the discretization using the CBS algorithm

We shall first consider the treatment of boundaries described under (1) or (2) of the previous section. On such boundaries

$$u_n = 0, \qquad \text{normal velocity zero} \tag{3.105}$$

and either

$$t_s = 0, \qquad \text{tangential traction zero for inviscid flow}$$

or

$$u_s = 0, \qquad \text{tangential velocity zero for viscous flow}$$

In early applications of the CBS algorithm it appeared correct that when computing $\Delta\tilde{U}_i^\star$ *no* velocity boundary conditions be imposed and to use instead the value of boundary tractions which corresponds to the deviatoric stresses and pressures computed at time $t_n$. We note that if the pressure is removed as in Split A these pressures could also be removed from the boundary traction component. However, in Split B no such pressure removal is necessary. This requires, in viscous problems, evaluation of the boundary $\tau_{ij}$'s and this point is explained further later.

When computing $\Delta\rho$ or $\Delta p$ we integrate by parts obtaining [Eq. (3.55)]

$$\begin{aligned}\int_\Omega N_p^k \frac{1}{c^2}\Delta p\,\mathrm{d}\Omega &= -\Delta t\int_\Omega N_p^k \frac{\partial}{\partial x_i}\left(U_i^n + \theta_1\Delta U_i^\star - \theta_1\Delta t\frac{\partial p^{n+\theta_2}}{\partial x_i}\right)\mathrm{d}\Omega\\ &= \Delta t\int_\Omega \frac{\partial N_p^k}{\partial x_i}\left[U_i^n + \theta_1\left(\Delta U_i^\star - \Delta t\frac{\partial p^{n+\theta_2}}{\partial x_i}\right)\right]d\omega\\ &\quad - \Delta t\int_\Gamma N_p^k n_i\left[U_i^n + \theta_1\left(\Delta U_i^\star - \Delta t\frac{\partial p^{n+\theta_2}}{\partial x_i}\right)\right]\mathrm{d}\Gamma \qquad (3.106)\end{aligned}$$

Here $n_i$ is the outward drawn normal. The last term in the above equation is identically equal to zero on boundaries in which slip and no-slip conditions are applied from the condition of Eq. (3.26):

$$U_n = n_i U_i = n_i\left[U_i^n + \theta_1\left(\Delta U_i^\star - \Delta t\frac{\partial p^{n+\theta_2}}{\partial x_i}\right)\right] = 0 \qquad (3.107)$$

For nonzero normal velocity this would simply become the specified normal velocity. This point seems to have baffled some investigators who simply assume

$$\frac{\partial p}{\partial n} = n_i\frac{\partial p}{\partial x_i} = 0 \qquad (3.108)$$

on solid boundaries although this is not exactly true as shown by Codina et al. [46].

Returning to the traction on the boundaries, the traction on the surface can be defined as

$$t_i = \tau_{ij}n_j - p\,n_i \qquad (3.109)$$

Prescribing the above traction using Split A, we replace the stress components in Step 1 [last term in Eq. (3.34)] as follows:

$$\int_\Gamma N_u^k\tau_{ij}n_j\,\mathrm{d}\Gamma = \int_{\Gamma-\Gamma_t} N_u^k\tau_{ij}n_j\,\mathrm{d}\Gamma + \int_{\Gamma_t} N_u^k(t_i + p\,n_i)\,\mathrm{d}\Gamma \qquad (3.110)$$

where $\Gamma_t$ represents the part of the boundary where the traction is prescribed.

The above calculation may involve a substantial error in "projecting" deviatoric stresses onto the boundary.

The last step requires the solution for the velocity correction terms to obtain finally the $\tilde{U}_i^{n+1}$. Clearly correct velocity boundary values must always be imposed in this step.

Although the above-described procedure is theoretically correct and instructive, it is complex to implement. For this reason we will recommend the use of a much simpler procedure which relies on the fact that when summation is made of the CBS components correct velocity and traction conditions should be satisfied by the sum. Thus in the recommended procedure we apply all the specified tractions.

## 3.10 The performance of two- and single-step algorithms on an inviscid problem

In this section we demonstrate the performance of the single- and two-step algorithms via an inviscid problem of subsonic and supersonic flow past a NACA0012 aerofoil. The problem domain and finite element mesh used are shown in Fig. 3.3a and b. The discretization near the aerofoil surface is finer than that of other places and a total number of 969 nodes and 1824 elements are used in the mesh.

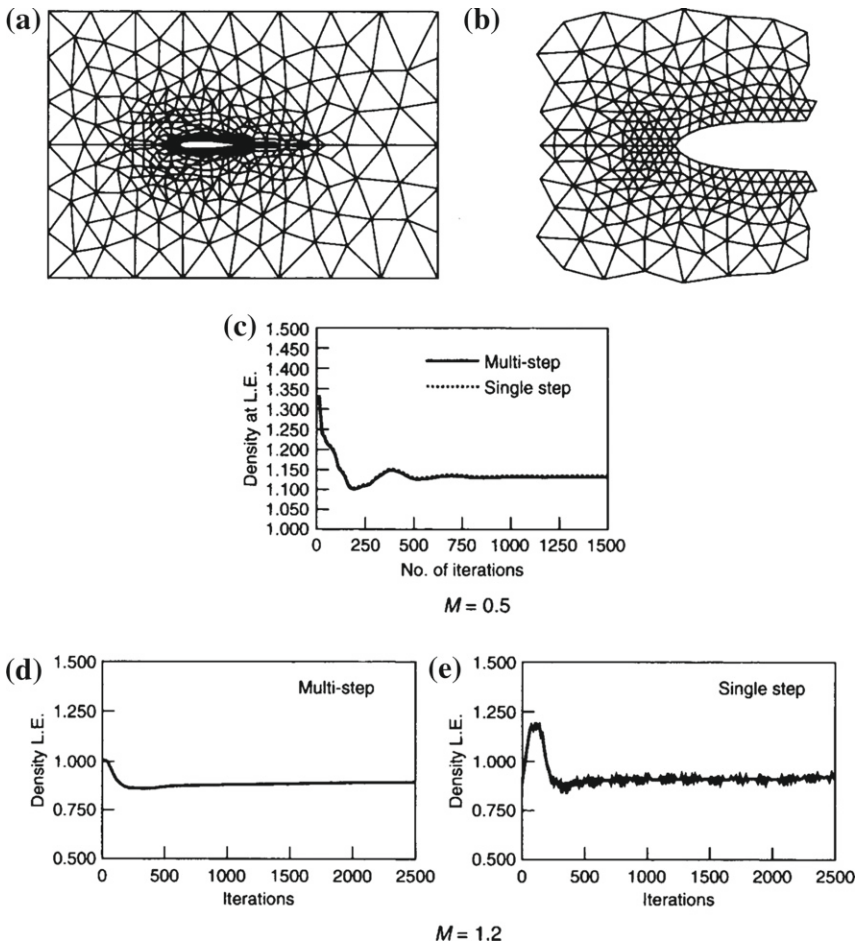


**FIGURE 3.3**

Inviscid flow past a NACA0012 aerofoil $\alpha = 0$: (a) unstructured mesh with 1824 elements and 969 nodes; (b) details of mesh near stagnation point; (c) steady-state convergence for $M = 0.5$ with two- and single-step schemes, fully explicit form; (d) steady-state convergence for $M = 1.2$ for two-step scheme; (e) steady-state convergence for $M = 1.2$ for single-step scheme.

The inlet Mach number is assumed to be equal to 0.5 and all variables except the density are prescribed at the inlet. The density is imposed at the exit of the domain. Both the top and bottom sides are assumed to be symmetric with normal component of velocity equal to zero. A slipping boundary is assumed on the surface of the aerofoil. No real or additional viscosity in any form is used in this problem when we use the CBS algorithm. However other schemes do need additional diffusions to get a reasonable solution.

Figure 3.3c shows the comparison of the density evolution at the stagnation point of the aerofoil. It is observed that the difference between the single- and two-step schemes is negligibly small. Further tests on these schemes were carried out at a higher inlet Mach number of 1.2 with the flow being supersonic, and a different mesh with a higher number of nodes (3753) and elements (7351). Here all the variables at the inlet were specified and the exit was free. As we can see from Fig. 3.3d and e, the single-step scheme gives spurious oscillations in density values at the stagnation

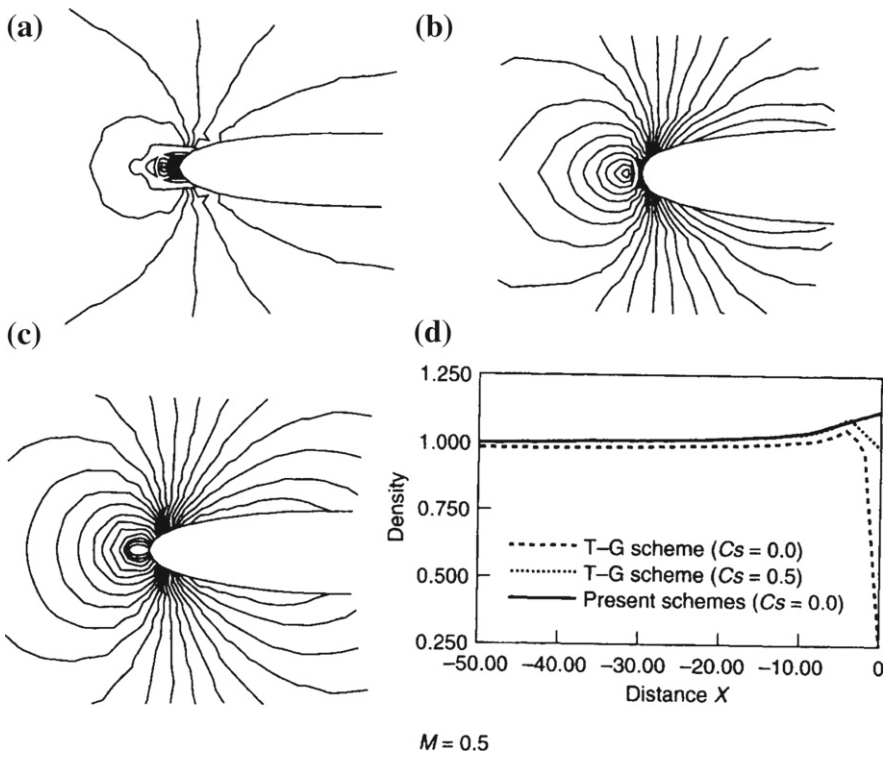


**FIGURE 3.4**

Subsonic inviscid flow past a NACA0012 aerofoil with $\alpha = 0$ and $M = 0.5$: (a) density contours with TG scheme with no additional viscosity; (b) density contours with TG scheme with additional viscosity; (c) density contours with CBS scheme with no additional viscosity; (d) comparison of density along the stagnation line.

point. Therefore we conclude that here the two-step algorithm is valid for any range of Mach numbers and the single-step algorithm is limited to low Mach numbers flows with small compressibility.

In Fig. 3.4 we compare the two-step algorithm results of the subsonic inviscid ($M = 0.5$) results with those obtained by the Taylor-Galerkin scheme for the same mesh. It is observed that the CBS algorithm gives a smooth solution near the stagnation point even though no additional artificial diffusion is introduced. However the Taylor-Galerkin scheme gives spurious solutions and a reasonable solution is obtained from this scheme only with a considerable amount of additional diffusion. Comparison of density distribution along the stagnation line shows (Fig. 3.4d) that the Taylor-Galerkin scheme gives an incorrect solution even with additional diffusion. However, the CBS algorithm again gives an accurate solution without the use of any additional artificial diffusion.

## 3.11 Performance of dual time stepping to remove pressure error

The problem considered here is to demonstrate that the performance of a quasi-implicit scheme with dual time stepping is vortex decay within a unit square domain. This analytical benchmark allows for a quantitative assessment of the relative temporal properties of the standard quasi-implicit scheme compared to that of dual time stepping–based approach. This two-dimensional problem has the following analytical solution:

$$\begin{aligned} u(x, y, t) &= -\cos \pi x \sin \pi y \exp^{-2\pi^2 t/Re} \\ v(x, y, t) &= \sin \pi x \cos \pi y \exp^{-2\pi^2 t/Re} \\ p(x, y, t) &= -\frac{1}{4}\left(\cos 2\pi x + \cos 2\pi y\right) \exp^{-4\pi^2 t/Re} \end{aligned} \tag{3.111}$$

where $Re = 20$ and $-0.5 \leq x, y \leq 0.5$. The initial and boundary conditions are computed using the analytical solution. The initial time history that is needed to enact the dual time stepping is also calculated using the analytical solution. A uniformly structured mesh of 115,200 linear triangular elements was employed in the calculations. The instantaneous steady-state convergence within the pseudo time stepping iteration loop was determined via a normalized L2 norm of the velocity and pressure differences between two consecutive pseudo time steps. In both cases, a tolerance of $1 \times 10^{-11}$ was employed.

In order to assess the temporal convergence behavior, the difference between the analytical solution and the predicted numerical solution was examined at a total time of unity. The difference between the analytical and predicted solutions was determined (e.g., for pressure) using

$$error = \frac{||p - p_{analytical}||}{||p_{analytical}||} \tag{3.112}$$

where ||.|| denotes the Euclidean norm. Once the error was determined for a range of transient time step values ($\Delta\tau$ values), a least-squares technique was utilized to determine the rate of convergence.

The convergence of the dual time-stepping approach is demonstrated in Fig. 3.5. In this figure, both velocity and pressure temporal behavior is identical. The calculated convergence in time is presented in Table 3.1 for both the classical and dual time-stepping approaches. As seen all calculated convergence gradients have a Pearson coefficient greater than 0.9992, demonstrating that a negligible error exists within the calculated convergence rates. It is very clear from Fig. 3.5 and Table 3.1 that dual time stepping gives the expected formal accuracy in time. This behavior demonstrates the monolithic equivalence of the dual time-stepping–based quasi-implicit scheme. However, since the scheme does not require a monolithic solution procedure, the computational cost is reduced.

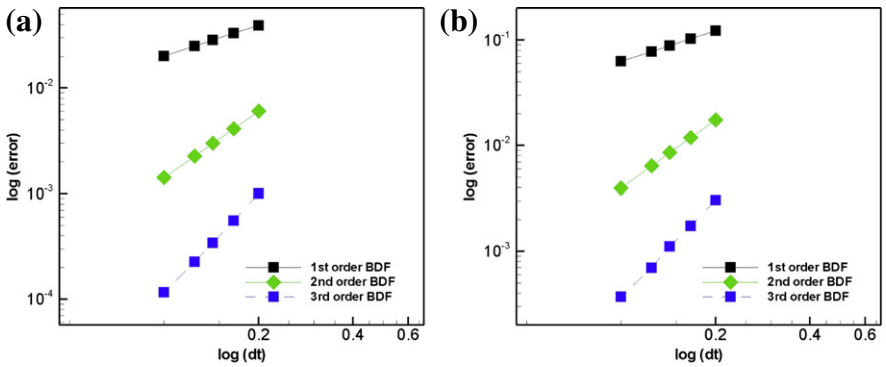


**FIGURE 3.5**

Vortex decay. Temporal convergence of the dual time-stepping quasi-implicit scheme with first-, second-, and third-order backward difference formula for $\Delta u^n/\Delta\tau$: (a) velocity; (b) pressure.

**Table 3.1** Vortex Decay: Calculated Rates of Convergence and Associated Pearson Coefficient

| Method | Order | Velocity | Pearson Coefficient (V) | Pressure | Pearson Coefficent (P) |
|---|---|---|---|---|---|
| Standard | 1st | 0.9038 | 0.9992 | 0.9561 | 1.0000 |
| Dual time | 1st | 0.9657 | 1.0000 | 0.9670 | 1.0000 |
| Standard | 2nd | 2.0339 | 0.9996 | 1.1512 | 0.9993 |
| Dual time | 2nd | 2.1426 | 1.0000 | 2.1334 | 0.9999 |
| Dual time | 3rd | 3.1146 | 0.9997 | 3.0608 | 0.9992 |

## 3.12 Concluding remarks

The general CBS algorithm is discussed in detail in this chapter for the equations of fluid dynamics in their conservation form. Comparison between the single- and two-step algorithms in section 3.10 shows that the latter scheme is valid for all ranges of flows. In later chapters, we generally apply the two-step algorithm for different flow applications. Another important conclusion made from this chapter is about the accuracy of the present scheme. As observed in section 3.10, the present CBS algorithm gives excellent performance when the flow is slightly compressible compared to the Taylor-Galerkin algorithm. In the following chapters we show further tests on the algorithm for a variety of problems including general compressible and incompressible flow problems, shallow-water problems, etc.

## References

[1] O.C. Zienkiewicz, R.L. Taylor, J.Z. Zhu, The Finite Element Method: Its Basis and Fundamentals, seventh ed., Elsevier, Oxford, 2013.

[2] I. Babuška, The finite element method with Lagrangian multipliers, Numer. Math. 20 (1973) 179–192.

[3] F. Brezzi, On the existence, uniqueness and approximation of saddle-point problems arising from Lagrange multipliers, Rev. Française d'Automatique Inform. Rech. Opér., Ser. Rouge Anal. Numér. 8 (R-2) (1974) 129–151.

[4] A.J. Chorin, Numerical solution of Navier-Stokes equations, Math. Comput. 22 (1968) 745–762.

[5] A.J. Chorin, On the convergence of discrete approximation to the Navier-Stokes equations, Math. Comput. 23 (1969) 341–353.

[6] G. Comini, S. Del Guidice, Finite element solution of incompressible Navier-Stokes equations, Numer. Heat Transfer, Part A 5 (1972) 463–478.

[7] G.E. Schneider, G.D. Raithby, M.M. Yovanovich, Finite element analysis of incompressible flow incorporating equal order pressure and velocity interpolation, in: C. Taylor, K. Morgan, C.A. Brebbia (Eds.), Numerical Methods in Laminar and Turbulent Flow, Pentech Press, Plymouth, 1978.

[8] J. Donea, S. Giuliani, H. Laval, L. Quartapelle, Finite element solution of unsteady Navier-Stokes equations by a fractional step method, Comput. Methods Appl. Mech. Eng. 33 (1982) 53–73.

[9] P.M. Gresho, S.T. Chan, R.L. Lee, C.D. Upson, A modified finite element method for solving incompressible Navier-Stokes equations. Part I: Theory, Int. J. Numer. Methods Eng. 4 (1984) 557–598.

[10] M. Kawahara, K. Ohmiya, Finite element analysis of density flow using the velocity correction method, Int. J. Numer. Methods Eng. 5 (1985) 981–993.

[11] J.G. Rice, R.J. Schnipke, An equal-order velocity-pressure formulation that does not exhibit spurious pressure modes, Comput. Methods Appl. Mech. Eng. 58 (1986) 135–149.

[12] B. Ramaswamy, M. Kawahara, T. Nakayama, Lagrangian finite element method for the analysis of two dimensional sloshing problems, Int. J. Numer. Methods Fluids 6 (1986) 659–670.
[13] B. Ramaswamy, Finite element solution for advection and natural convection flows, Comput. Fluids 16 (1988) 349–388.
[14] M. Shimura, M. Kawahara, Two dimensional finite element flow analysis using the velocity correction procedure, Earthq. Eng. Struct. Dyn. 5 (1988) 255–263.
[15] S.G.R. Kumar, P.A.A. Narayana, K.N. Seetharamu, B. Ramaswamy, Laminar flow and heat transfer over a two dimensional triangular step, Int. J. Numer. Methods Fluids 9 (1989) 1165–1177.
[16] B. Ramaswamy, T.C. Jue, J.E. Akin, Semi-implicit and explicit finite element schemes for coupled fluid thermal problems, Int. J. Numer. Methods Eng. 34 (1992) 675–696.
[17] R. Rannacher, On Chorin's projection method for the incompressible Navier-Stokes equations, Lect. Notes Math. 1530 (1993) 167–183.
[18] B. Ramaswamy, Theory and implementation of a semi-implicit finite element method for viscous incompressible flows, Comput. Fluids 22 (1993) 725–747.
[19] C.B. Yiang, M. Kawahara, A three step finite element method for unsteady incompressible flows, Comput. Mech. 11 (1993) 355–370.
[20] G. Ren, T. Utnes, A finite element solution of the time dependent incompressible Navier-Stokes equations using a modified velocity correction method, Int. J. Numer. Methods Fluids 17 (1993) 349–364.
[21] B.V.K.S. Sai, K.N. Seetharamu, P.A.A. Narayana, Solution of transient laminar natural convection in a square cavity by an explicit finite element scheme, Numer. Heat Transfer, Part A 25 (1994) 593–609.
[22] M. Srinivas, M.S. Ravisanker, K.N. Seetharamu, P.A. Aswathanarayana, Finite element analysis of internal flows with heat transfer, Sadhana - Acad. Proc. Eng. 19 (1994) 785–816.
[23] P.M. Gresho, S.T. Chan, M.A. Christon, A.C. Hindmarsh, A little more on stabilized Q1Q1 for transient viscous incompressible flow, Int. J. Numer. Methods Fluids 21 (1995) 837–856.
[24] Y.T.K. Gowda, P.A.A. Narayana, K.N. Seetharamu, Mixed convection heat transfer past in-line cylinders in a vertical duct, Numer. Heat Transfer, Part A 31 (1996) 551–562.
[25] A.R. Chaudhuri, K.N. Seetharamu, T. Sundararajan, Modelling of steam surface condenser using finite element methods, Commun. Appl. Numer. Methods 13 (1997) 909–921.
[26] P. Nithiarasu, T. Sundararajan, K.N. Seetharamu, Finite element analysis of transient natural convection in an odd-shaped enclosure, Int. J. Num. Methods Heat Fluid Flow 8 (1998) 199–220.
[27] P.K. Maji, G. Biswas, Three-dimensional analysis of flow in the spiral casing of a reaction turbine using a differently weighted Petrov Galerkin method, Comput. Methods Appl. Mech. Eng. 167 (1998) 167–190.

[28] P.D. Minev, P.M. Gresho, A remark on pressure correction schemes for transient viscous incompressible flow, Commun. Appl. Numer. Methods 14 (1998) 335–346.
[29] J. Blasco, R. Codina, A. Huerta, A fractional-step method for the incompressible Navier-Stokes equations related to a predictor-multicorrector algorithm, Int. J. Numer. Methods Fluids 28 (1998) 1391–1419.
[30] B.S.V.P. Patnaik, P.A.A. Narayana, K.N. Seetharamu, Numerical simulation of vortex shedding past a cylinder under the influence of buoyancy, Int. J. Heat Mass Transfer 42 (1999) 3495–3507.
[31] J.L. Guermond, Result of convergence of order two in time for approximation of Navier-Stokes equations by means of an incremental projection method, RAIRO - Mathematical Modelling and Numerical Analysis 33 (1999) 169–189.
[32] J.L. Guermond, J. Shen, Velocity-correction projection methods for incompressible flows, SIAM J. Numer. Anal. 41 (2003) 112–134.
[33] J.L. Guermond, P. Minev, J. Shen, An overview of projection methods for incompressible flows, Comput. Methods Appl. Mech. Eng. 195 (44–47) (2006) 6011–6045.
[34] S. Dong, J. Shen, An unconditionally stable rotational velocity-correction scheme for incompressible flows, J. Comput. Phys. 229 (19) (2010) 7013–7029.
[35] O.C. Zienkiewicz, R. Codina, Search for a general fluid mechanics algorithm, in: D.A. Caughey, M.M. Hafez (Eds.), Frontiers of Computational Fluid Dynamics, John Wiley & Sons, New York, 1995, pp. 101–113.
[36] O.C. Zienkiewicz, R. Codina, A general algorithm for compressible and incompressible flow—Part I: The split, characteristic-based scheme, Int. J. Numer. Methods Fluids 20 (1995) 869–885.
[37] O.C. Zienkiewicz, B.V.K.S. Sai, K. Morgan, R. Codina, M. Vázquez, A general algorithm for compressible and incompressible flow—Part II: Tests on the explicit form, Int. J. Numer. Methods Fluids 20 (1995) 887–913.
[38] O.C. Zienkiewicz, P. Ortiz, A split characteristic based finite element model for shallow water equations, Int. J. Numer. Methods Fluids 20 (1995) 1061–1080.
[39] P. Ortiz, O.C. Zienkiewicz, Modelizacin por elementos finitos en hidrulica e hidrodinmica costera, Technical report, Centro de Estudios y Experimentation de Obras Pblicas, CEDEX, Madrid, 1995.
[40] O.C. Zienkiewicz, A new algorithm for fluid mechanics. Compressible and incompressible behaviour, in: M. Morandi Cecchi, K. Morgan, J. Periaux, B.A. Schrefler, O.C. Zienkiewicz (Eds.), Proceedings of the 9th International Conference on Finite Elements Fluids—New Trends and Applications, Venezia, October 1995, pp. 49–55.
[41] R. Codina, M. Vázquez, O.C. Zienkiewicz, A fractional step method for compressible flows: boundary conditions and incompressible limit, in: M. Morandi Cecchi, K. Morgan, J. Periaux, B.A. Schrefler, O.C. Zienkiewicz (Eds.), Proceedings of the 9th International Conference on Finite Elements Fluids—New Trends and Applications, Venezia, October 1995, pp. 409–418.

[42] P. Ortiz, O.C. Zienkiewicz, Tide and bore propagation in the Severn Estuary by a new algorithm, in: M. Morandi Cecchi, K. Morgan, J. Periaux, B.A. Schrefler, O.C. Zienkiewicz (Eds.), Proceedings of the 9th International Conference on Finite Elements Fluids—New Trends and Applications, Venezia, October 1995, pp. 1543–1552.
[43] O.C. Zienkiewicz, B.V.K.S. Sai, K. Morgan, R. Codina, Split characteristic based semi-implicit algorithm for laminar/turbulent incompressible flows, Int. J. Numer. Methods Fluids 23 (1996) 1–23.
[44] P. Ortiz, O.C. Zienkiewicz, An improved finite element model for shallow water problems, in: G.F. Carey (Ed.), Finite Element Modeling of Environmental Problems, John Wiley & Sons, New York, 1996, pp. 61–84.
[45] P. Nithiarasu, O.C. Zienkiewicz, B.V.K.S. Sai, K. Morgan, R. Codina, M. Vázquez, Shock capturing viscosities for the general fluid mechanics algorithm, Int. J. Numer. Methods Fluids 28 (1998) 1325–1353.
[46] R. Codina, M. Vázquez, O.C. Zienkiewicz, General algorithm for compressible and incompressible flows, Part III—A semi-implicit form, Int. J. Numer. Methods Fluids 27 (1998) 13–32.
[47] B.V.K.S. Sai, O.C. Zienkiewicz, M.T. Manzari, P.R.M. Lyra, K. Morgan, General purpose vs. special algorithms for high speed flows with shocks, Int. J. Numer. Methods Fluids 27 (1998) 57–80.
[48] R. Codina, M. Vázquez, O.C. Zienkiewicz, A fractional step method for the solution of compressible Navier-Stokes equations, in: M. Hafez, K. Oshima (Eds.), Computational Fluid Dynamics Review 1998, vol. 1, World Scientific Publishing, 1998, pp. 331–347.
[49] N. Massarotti, P. Nithiarasu, O.C. Zienkiewicz, Characteristic-based-split (CBS) algorithm for incompressible flow problems with heat transfer, Int. J. Numer. Methods Heat Fluid Flow 8 (1998) 969–990.
[50] O.C. Zienkiewicz, P. Nithiarasu, R. Codina, M. Vázquez, P. Ortiz, Characteristic-based-split algorithm, Part I: The theory and general discussion, in: K.D. Papailou et al. (Eds.), Proceedings of the ECCOMAS CVD 1998, vol. 2, 1998, Greece, Athens
[51] N. Massarotti, P. Nithiarasu, O.C. Zienkiewicz, Characteristic-based-split algorithm, Part II: Incompressible flow problems with heat transfer, in: K.D. Papailou et al. (Eds.), Proceedings of ECCOMAS CFD 1998, vol. 2, 1998, Greece, Athens
[52] O.C. Zienkiewicz, P. Ortiz, The CBS (characteristic-based-split) algorithm in hydraulic and shallow water flow, in: Proceedings of the Second International Symposium on Environmental Hydraulics, University of Hong Kong, December 1998, pp. 3–12.
[53] P. Nithiarasu, O.C. Zienkiewicz, On stabilization of the CBS algorithm. Internal and external time steps, Int. J. Numer. Methods Eng. 48 (2000) 875–880.
[54] O.C. Zienkiewicz, J. Rojek, R.L. Taylor, M. Pastor, Triangles and tetrahedra in explicit dynamic codes for solids, Int. J. Numer. Methods Eng. 43 (1999) 565–583.

[55] O.C. Zienkiewicz, P. Nithiarasu, R. Codina, M. Vázquez, The characteristic based split procedure: an efficient and accurate algorithm for fluid problems, Int. J. Numer. Methods Fluids 31 (1999) 359–392.
[56] P. Nithiarasu, Boundary conditions for the characteristic based split (CBS) algorithm for fluid dynamics, Int. J. Numer. Methods Eng. 54 (2002) 523–536.
[57] P. Nithiarasu, An efficient artificial compressibility (AC) scheme based on the characteristic based split (CBS) method for incompressible flows, Int. J. Numer. Methods Eng. 56 (2003) 1815–1845.
[58] P. Nithiarasu, J.S. Mathur, N.P. Weatherill, K. Morgan, Three-dimensional incompressible flow calculations using the characteristic based split (CBS) scheme, Int. J. Numer. Methods Fluids 44 (2004) 1207–1229.
[59] P. Nithiarasu, N. Massarotti, J.S. Mathur, Forced convection heat transfer heat from solder balls on a printed circuit board using the characteristic based split (CBS) scheme, Int. J. Numer. Methods Heat Fluid Flow 15 (1) (2005) 73–95.
[60] P. Nithiarasu, An arbitrary Lagrangian Eulerian (ALE) formulation for free surface flows using the characteristic-based split (CBS) scheme, Int. J. Numer. Methods Fluids 48 (2005) 1415–1428.
[61] P. Nithiarasu, C.-B. Liu, Steady and unsteady incompressible flow in a double driven cavity using the artificial compressibility (AC)-based characteristic-based split (CBS) scheme, Int. J. Numer. Methods Eng. 63 (2005) 380–397.
[62] P. Nithiarasu, R. Codina, Special issue: Characteristic-based split (CBS) procedure, Int. J. Numer. Methods Eng. 66 (2006) 1511–1512.
[63] X. Li, Q. Duan, Meshfree iterative stabilized Taylor-Galerkin and characteristic-based split (CBS) algorithms for incompressible N-S equations, Comput. Methods Appl. Mech. Eng. 195 (2006) 6125–6145.
[64] P. Nithiarasu, C.-B. Liu, An artificial compressibility based characteristic based split (CBS) scheme for steady and unsteady turbulent incompressible flows, Comput. Methods Appl. Mech. Eng. 195 (2006) 2961–2982.
[65] O.C. Zienkiewicz, Special issue: Characteristic-based split (CBS) procedure—Foreword, Int. J. Numer. Methods Eng. 66 (2006) 1513.
[66] V.M. Kulkarni, K.N. Seetharamu, I.A. Azid, P.A.A. Narayana, G.A. Quadir, Numerical simulation of underfill encapsulation process based on characteristic split method, Int. J. Numer. Methods Eng. 66 (2006) 1658–1671.
[67] M. Morandi-Cecchi, M. Venturin, Characteristic-based split (CBS) algorithm finite element modelling for shallow waters in the Venice lagoon, Int. J. Numer. Methods Eng. 66 (2006) 1641–1657.
[68] P. Nithiarasu, R. Codina, O.C. Zienkiewicz, The characteristic-based split (CBS) scheme—a unified approach to fluid dynamics, Int. J. Numer. Methods Eng. 66 (2006) 1514–1546.
[69] P. Nithiarasu, C.-B. Liu, N. Massarotti, Laminar and turbulent flow calculations through a model human upper airway using unstructured meshes , Commun. Numer. Methods Eng. 23 (12) (2007) 1057–1069.

[70] C.-B. Liu, P. Nithiarasu, The characteristic-based split (CBS) scheme for viscoelastic flow past a circular cylinder, Int. J. Numer. Methods Fluids 57 (2008) 157–176.
[71] C.-B. Liu, P. Nithiarasu, An artificial-dissipation-based fractional step scheme for upper-convected Maxwell (UCM) fluid flow past a circular cylinder, Int. J. Numer. Methods Fluids 57 (2008) 1171–1187.
[72] P. Nithiarasu, O. Hassan, K. Morgan, N.P. Weatherill, C. Fielder, H. Whittet, P. Ebden, K.R. Lewis, Steady flow through a realistic human upper airway geometry, Int. J. Numer. Methods Fluids 57 (2008) 631–651.
[73] K. Chitra, S. Vengadesan, T. Sundararajan, P. Nithiarasu, An investigation of pulsatile flow in a model cavo-pulmonary vascular system, Commun. Numer. Methods Eng. 25 (2009) 1061–1083.
[74] Y. Bao, D. Zhou, C. Huang, Numerical simulation of flow over three circular cylinders in equilateral arrangements at low Reynolds number by a second-order characteristic-based split finite element method, Comput. Fluids 39 (2010) 882–899.
[75] R.L.T. Bevan, P. Nithiarasu, R. Van Loon, I. Sazonov, H. Luckraz, A. Garnham, Application of a locally conservative Galerkin (LCG) method for modelling blood flow through a patient-specific carotid bifurcation, Int. J. Numer. Methods Fluids 64 (2010) 1274–1295.
[76] X. H Zhang, J. Ouyang, L. Zhang, The characteristic-based split (CBS) meshfree method for free surface flow problems in ALE formulation, Int. J. Numer. Methods Fluids 65 (2011) 798–811.
[77] A. Mauro, P. Nithiarasu, N. Massarotti, F. Arpino, The finite element method: discretization and application to heat convection problems, in: R.S. Amano, B. Sunden (Eds.), Computational Fluid Dynamics and Heat Transfer: Emerging Topics, International Series on Developments in Heat Transfer, WIT Press, Billerica, MA, 2011, pp. 129–170.
[78] R.L.T. Bevan, I. Sazonov, P.H. Saksono, P. Nithiarasu, R. van Loon, H. Luckraz, S. Ashraf, Patient-specific blood flow simulation through an aneurysmal thoracic aorta with a folded proximal neck, Int. J. Numer. Methods Biomed. Eng. 27 (2011) 1167–1184.
[79] P.H. Saksono, P. Nithiarasu, I. Sazonov, S.Y. Yeo, Computational flow studies in a subject-specific human upper airway using a one-equation turbulence model. Influence of the nasal cavity, Int. J. Numer. Methods Eng. 87 (2011) 96–114.
[80] K. Chitra, T. Sundararajan, S. Vengadesan, P. Nithiarasu, Non-Newtonian blood flow study in a model cavopulmonary vascular system, Int. J. Numer. Methods Fluids 66 (2011) 269–283.
[81] P. Nithiarasu, R. Bevan, I. Sazonov, R. van Loon, H. Luckraz, M. Collins, A. Garnham, Influences of domain extensions to a moderately stenosed patient-specific carotid bifurcation: Investigation of wall quantities, Int. J. Numer. Methods Heat Fluid Flow 21 (2011) 952–979.

[82] P.H. Saksono, P. Nithiarasu, I. Sazonov, Numerical prediction of heat transfer patterns in a subject-specific human upper airway, J. Heat Transfer—Trans. ASME 134 (2012).
[83] R.L.T. Bevan, P. Nithiarasu, Accelerating incompressible flow calculations using a quasi-implicit scheme: local and dual time stepping approaches, Comput. Mech. 50 (6, SI) (2012) 687–693.
[84] R.L.T. Bevan, R.W. Lewis, P. Nithiarasu, Forced convection heat transfer within a moderately-stenosed, patient-specific carotid bifurcation, Int. J. Numer. Methods Heat Fluid Flow 22 (2012) 1120–1134.
[85] C.A. Klettner, I. Eames, Viscous free surface simulations with the characteristic based split scheme, Comput. Fluids 71 (2013) 487–495.
[86] F. Arpino, N. Massarotti, A. Mauro, P. Nithiarasu, Artificial compressibility based CBS solutions for double diffusive natural convection in cavities, Int. J. Numer. Methods Heat Fluid Flow 23 (2013) 205–225.
[87] P. Nithiarasu, R.L.T. Bevan, K. Murali, An artificial compressibility based fractional step method for solving time dependent incompressible flow equations. Temporal accuracy and similarity with a monolithic method, Comput. Mech. 51 (3) (2013) 255–260.
[88] O.C. Zienkiewicz, J. Szmelter, J. Peraire, Compressible and incompressible flow: an algorithm for all seasons, Comput. Methods Appl. Mech. Eng. 78 (1990) 105–121.
[89] O.C. Zienkiewicz, Explicit or semi-explicit general algorithm for compressible and incompressible flows with equal finite element interpolation, Technical Report 90/5, Chalmers Technical University, Gothenburg, 1990.
[90] O.C. Zienkiewicz, Finite elements and computational fluid mechanics, in: SEMNI Congress, Metodos Numericos en Ingenieria, Gran Canaria, 1991, pp. 51–61.
[91] O.C. Zienkiewicz, J. Wu, Incompressibility without tears! How to avoid restrictions of mixed formulations, Int. J. Numer. Methods Eng. 32 (1991) 1184–1203.
[92] O.C. Zienkiewicz, J. Wu, A general explicit or semi-explicit algorithm for compressible and incompressible flows, Int. J. Numer. Methods Eng. 35 (1992) 457–479.
[93] P. Nithiarasu, O.C. Zienkiewicz, Analysis of an explicit and matrix free fractional step method for incompressible flows, Comput. Methods Appl. Mech. Eng. 195 (41–43) (2006) 5537–5551.
[94] C. Thomas, P. Nithiarasu, The characteristic based split (CBS) approach for inviscid compressible flow problems. Effect of element size calculation in the streamline direction, in: Netanmaki et al. (Eds.), ECCOMAS, 2004, Jyväskylä, Finland, 24-28 July, 2004.
[95] O.C. Zienkiewicz, S. Qu, R.L. Taylor, S. Nakazawa, The patch test for mixed formulations, Int. J. Numer. Methods Eng. 23 (1986) 1873–1883.
[96] O.C. Zienkiewicz, R.L. Taylor, The finite element patch test revisited: a computer test for convergence, validation and error estimates, Comput. Methods Appl. Mech. Eng. 149 (1997) 523–544.

[97] A. Jameson, D.J. Mavripolis, Finite volume solution of the two dimensional Euler equations on a regular triangular mesh, in: AIAA 23th Aerospace Sciences Meeting, Reno, NV, 1985, Paper AIAA-85-0435.
[98] F. Brezzi, J. Pitkäranta, On the stabilization of finite element approximations of the Stokes problem, in: W. Hackbusch (Ed.), Efficient Solution of Elliptic Problems, Notes on Numerical Fluid Mechanics, vol. 10, Vieweg, Wiesbaden, 1984.
[99] J. Kim, P. Moin, Application of a fractional step method to incompressible Navier-Stokes equations, J. Comput. Phys. 59 (1985) 308–323.
[100] J.B. Perot, An analysis of the fractional step method, J. Comput. Phys. 108 (1993) 51–58.
[101] R. Codina, Pressure stability in fractional step finite element methods for incompressible flows, J. Comput. Phys. 170 (2001) 112–140.
[102] T.M. Burton, J.K. Eaton, Analysis of a fractional-step method on overset grids, J. Comput. Phys. 177 (2002) 336–364.
[103] T.C. Papanastasiou, N. Malamataris, K. Ellwood, A new outflow boundary condition, Int. J. Numer. Methods Fluids 14 (1992) 587–608.